



Projections of water, carbon, and nitrogen dynamics under future climate change in an old-growth Douglas-fir forest in the western Cascade Range using a biogeochemical model

Zheng Dong ^{a,*}, Charles T. Driscoll ^a, Sherri L. Johnson ^b, John L. Campbell ^c, Afshin Pourmokhtarian ^d, Anne M.K. Stoner ^e, Katharine Hayhoe ^e

^a Department of Civil and Environmental Engineering, Syracuse University, Syracuse, NY 13244, USA

^b Pacific Northwest Research Station, U.S. Forest Service, Corvallis, OR 97331, USA

^c Northern Research Station, U.S. Forest Service, Durham, NH 03824, USA

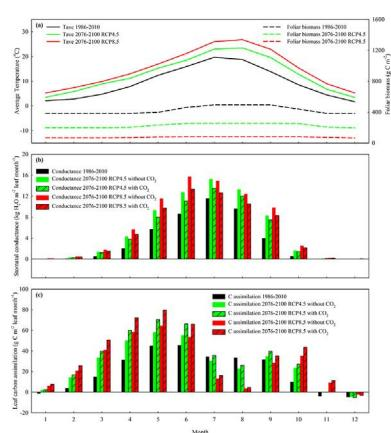
^d Department of Construction Management, Wentworth Institute of Technology, Boston, MA 02115, USA

^e Climate Science Center, Texas Tech University, Lubbock, TX 79409, USA

HIGHLIGHTS

- Element dynamics projected in an old-growth Douglas-fir forest under RCP scenarios
- Future increasing temperature causes severe physiological stress on the vegetation
- Decreasing photosynthesis, plant biomass, and soil organic matter are projected
- Projected mortality decreases transpiration and slightly increases soil moisture
- Future climate change alters foliar and soil carbon to nitrogen stoichiometry

GRAPHICAL ABSTRACT



ARTICLE INFO

Article history:

Received 17 September 2018

Received in revised form 19 November 2018

Accepted 25 November 2018

Available online 27 November 2018

Editor: Elena Paoletti

Keywords:

Douglas-fir

Representative concentration pathways

Biogeochemical modeling

Water

ABSTRACT

Statistically downscaled climate change scenarios from four General Circulation Models for two Representative Concentration Pathways (RCP) were applied as inputs to a biogeochemical model, PnET-BGC, to examine potential future dynamics of water, carbon, and nitrogen in an old-growth Douglas-fir forest in the western Cascade Range. Projections show 56% to 77% increases in stomatal conductance throughout the year from 1986–2010 to 2076–2100, and 65% to 104% increases in leaf carbon assimilation between October and June over the same period. However, future dynamics of water and carbon under the RCP scenarios are affected by a 49% to 86% reduction in foliar biomass resulting from severe air temperature and humidity stress to the forest in summer. Important implications of future decreases in foliar biomass include 1) 20% to 71% decreases in annual transpiration which increase soil moisture by 7% to 15% in summer and fall; 2) decreases in photosynthesis by 77% and soil organic matter by 62% under the high radiative forcing scenario; and 3) altered foliar and soil carbon to nitrogen stoichiometry. Potential carbon dioxide fertilization effects on vegetation are projected to 1) amplify decreases in transpiration by 4% to 9% and increases in soil moisture in summer and fall by 1% to 2%; and 2) alleviate

* Corresponding author.

E-mail address: zdong03@syr.edu (Z. Dong).



decreases in photosynthesis by 4%; while 3) having negligible effects on the dynamics of nitrogen. Our projections suggest that future decrease in transpiration and moderate water holding capacity may mitigate soil moisture stress to the old-growth Douglas-fir forest. Future increases in nitrogen concentration in soil organic matter are projected to alleviate the decrease in net nitrogen mineralization despite a reduction in decomposition of soil organic matter by the end of the century.

© 2018 Elsevier B.V. All rights reserved.

1. Introduction

Greenhouse gas emissions have substantially altered global climate (Bindoff et al., 2013). For example, in the Pacific Northwest, USA, annual mean temperature is projected to increase by 1.1 °C to 4.7 °C, while annual precipitation is projected to change by −4.7% to +13.5% from 1950–1999 to 2041–2070 under future radiative forcing scenarios of the Representative Concentration Pathways (RCP) assessed by the Intergovernmental Panel on Climate Change (IPCC) (Mote et al., 2013).

Evergreen coniferous forests in the Pacific Northwest are unique among temperate forests of the world in terms of their productivity and stand age, having adapted to the temperature, moisture, and nutrient regimes of the region (Waring and Franklin, 1979). Common species of conifers in the region such as Douglas-fir (*Pseudotsuga menziesii*) and western hemlock (*Tsuga heterophylla*) are among the world's most important and valuable timber trees (Burns and Honkala, 1990), and are widely distributed both in their native range from the Rocky Mountains to the Pacific Coast of North America as well as in many temperate regions of Europe (Hermann, 1987). Altered climate has caused widespread drought and heat-and-moisture-induced changes in ecosystem productivity (Allen et al., 2010; Boisvenue and Running, 2006) and soil respiration (Bond-Lamberty and Thomson, 2010). These climate effects can change carbon (C) storage and fluxes that alters the stoichiometry of litter and soil (Manzoni et al., 2008) and nitrogen (N) storage in vegetation and soil, and plant growth (Wieder et al., 2015). Under future climate change scenarios, increases in temperature and atmospheric CO₂ concentration coupled with changing precipitation are anticipated to substantially alter forest ecosystem function through changes in water balances and C and N cycling (Coops et al., 2010; Griesbauer and Green, 2010b; Latta et al., 2010).

Warming, moisture manipulation, and CO₂ fertilization experiments, as well as observations along elevational gradients to investigate impacts of climate change on future ecosystem dynamics have intrinsic limitations. The period of experimentation (years to decades) may be too short to reveal long-term changes in ecosystem function. Rapid changes in controlled climatic or environmental factors associated with experiments fail to depict the gradual chronic changes of future climate. Finally, climatic factors such as temperature may not be altered synchronously with other conditions such as precipitation or atmospheric CO₂ in experiments or gradient studies to represent actual future conditions. Modeling can be an effective tool to address these limitations in observational approaches. Ecosystem models have been increasingly coupled with remote sensing at regional and continental scales to investigate responses to global change, taking advantage of the smaller uncertainty in climate projections at larger scales. However, modeling studies at larger spatial scales have the disadvantage that long-term observations from multiple locations are often lacking to calibrate and test the models. Moreover, physiological processes that operate at larger scales are less well understood than those at smaller scales. Previous modeling studies of the impacts of climate change on the Pacific Northwest have focused on land cover and land use (Turner et al., 2015) or species distributions (Coops and Waring, 2011). There have been limited applications of ecosystem models to assess changes in water and element dynamics under climate change scenarios in this region (Hartman et al., 2014).

We used a deterministic biogeochemical model, PnET-BGC, driven by downscaled future climate scenarios from the fifth IPCC Assessment

Report (AR5) to assess biogeochemical impacts of climate change at a small intensively studied watershed in the western Cascade Range of the Pacific Northwest, USA. Our major objectives were to examine how changes in climatic factors might drive future dynamics in watershed processing of water, C, and N under the RCP scenarios in an old-growth Douglas-fir and western hemlock forest with Mediterranean climate, and to investigate potential effects of increases in atmospheric CO₂ on future ecosystem productivity and function.

In this study, we aim to address research questions on 1) what type (s) of physiological stress vegetation in the old-growth Douglas-fir forest might experience from climate change under the RCP scenarios; 2) to what extent might future increases in atmospheric CO₂ concentrations alleviate the impacts of these stresses; and 3) to what extent might physiological stresses affect the future dynamics of water, C, and N in this ecosystem. More specifically, our objectives are to examine the effects of changing air temperature, air humidity, soil moisture, and atmospheric carbon dioxide under the RCP scenarios on carbon sequestration, allocation, and productivity, and to elucidate consequent impacts on litterfall, decomposition of soil organic matter, N mineralization and uptake, and foliar and soil C to N stoichiometry. The intrinsic limitation in the nature of deductive reasoning precludes models to discover novel explanatory variables for current or future biogeochemical patterns. As a result, the goal of this research was to quantitatively examine the effects of multiple climatic and environmental factors that are gradually changing over the long-term on the future biogeochemistry of the Northwest forest. This was achieved by incorporating understanding and synthesizing up-to-date knowledge on ecosystem function into the algorithms and parameters of the process-based model. Note that our goal is not to predict the future, but rather to help manage uncertainty by narrowing the possible range to a subset of plausible futures that pertain directly to vulnerabilities of specific resources and management objectives (Littell et al., 2011). Our simulations are used to examine general biogeochemical principles rather than predict the behavior of a specific ecosystem (Green and Sadedin, 2005). For this reason, we use the term projection, not prediction, when describing the simulated model outputs about the future.

2. Materials and methods

2.1. Site description

The H.J. Andrews Experimental Forest (HJA), located in the western Cascade Range of Oregon, USA, covers the entire 6400 ha watershed of Lookout Creek. It has mountainous terrain with elevation ranging from 410 to 1630 m (Berntsen and Rothacher, 1959). The Mediterranean climate at HJA is characterized by wet, mild winters and dry, cool summers and is representative of the maritime Pacific Northwest (Bierlmaier and McKee, 1989). Previous research on ecosystem structure and function, nutrient dynamics, and forest-stream interactions have resulted in long-term ecological records that date back to the 1950s, providing detailed data for PnET-BGC model inputs, parameterization, calibration, and testing.

This study was conducted using data from Watershed 2, a 500-year old-growth forest at the HJA. Long-term measurements of meteorology, vegetation dynamics, and stream discharge and water chemistry are available for the watershed, as well as extensive records of soil properties from several surveys. Watershed 2 is north-facing with elevation

ranging from 545 to 1079 m (Valentine and Lienkaemper, 2005). As a result of the orographic pattern in temperature and precipitation, snowpack primarily occurs at the highest elevation of the watershed from November to March. Dominant overstory tree species at Watershed 2 include Douglas-fir (*Pseudotsuga menziesii*) and western hemlock (*Tsuga heterophylla*), and understory vegetation species include rhododendron (*Rhododendron macrophyllum*), vine maple (*Acer circinatum*), and sword-fern (*Polystichum munitum*) (Hawk and Dyrness, 1972).

2.2. Model structure

Developed from its predecessors PnET, PnET-II, PnET-Day, and PnET-CN, PnET-BGC includes a biogeochemical sub-model that allows for the simultaneous simulation of pools and fluxes of 10 major elements (Gbondo-Tugbawa et al., 2001) (Fig. 1). Different variations of the PnET model have been applied to study ecosystem responses to land disturbance, atmospheric deposition, and climate change (Braswell et al., 2005; Dong et al., 2018; Giltrap et al., 2010; Katsuyama et al., 2009; Pourmokhtarian et al., 2012; Pourmokhtarian et al., 2017; Richardson et al., 2007; Sacks et al., 2007; Thorn et al., 2015; Wallman et al., 2005). Potential CO₂ fertilization effects on vegetation can be either excluded or depicted in the model (Ollinger et al., 2009). PnET-BGC uses time-series inputs of solar radiation, temperature, precipitation, and atmospheric CO₂ concentration in a monthly time step to simulate the hydrologic and biogeochemical function of vegetation which affects the dynamics of soil and surface waters. The model also uses monthly wet atmospheric deposition and constant dry to wet deposition ratios of 10 elements as inputs. Plant functional traits are parameterized as vegetation type-specific values in PnET-BGC. Relative concentrations of elements to N in soil organic matter (SOM) and vegetation are also considered as fixed parameters.

PnET-BGC calculates photosynthetic rates per unit of leaf area based on foliar N contents and environmental stress to plants from air temperature, humidity, and soil moisture. Maximum net photosynthetic rates is calculated as a linear function of foliar N concentration using observed

relationship from the literature (Lewis et al., 2004; Reich, 2014; Ripullone et al., 2003; Wright et al., 2004). Gross photosynthetic rate considers an additional 10% basal foliar respiration modified by a Q₁₀ factor of 2 using 20 °C as the reference temperature (Aber, 1992). The degree of stress by air temperature, air humidity, and soil moisture are quantified by indices ranging from 0 to 1. The value of 1 is reached when air temperature is optimal for photosynthesis, vapor pressure deficit is 0 kpa, and the rate of actual transpiration equals the rate of potential transpiration (Aber, 1992),

$$NetPsn_{max} = AmaxA + AmaxB * FolNcon \quad (1)$$

$$GrossPsn_{max} = NetPsn_{max} * (1 + BaseFolResp) * Q_{10}^{\frac{(T_{day} - 20)}{10}} \quad (2)$$

$$GrossPsn = GrossPsn_{max} * DTTemp * DVVPD * DWater \quad (3)$$

$$DTTemp = \frac{(PsnT_{max} - T_{day}) * (T_{day} - PsnT_{min})}{\left(\frac{PsnT_{max} - PsnT_{min}}{2}\right)^2} \quad (4)$$

$$DVVPD = 1 - DVVPD1 * VPD^{DVVPD2} \quad (5)$$

where $NetPsn_{max}$ is the maximum net photosynthetic rate; $FolNcon$ is the foliar N concentration; $AmaxA$ and $AmaxB$ are constants representing the intercept and slope of relationship between $FolNcon$ and $NetPsn_{max}$; $GrossPsn_{max}$ and $GrossPsn$ are the maximum and actual gross photosynthetic rate; $BaseFolResp$ equals 10% and represents percentage basal foliar respiration at 20 °C; $DTTemp$ and $DVVPD$ are the indices for air temperature stress and air humidity stress (ranging from 0 to 1); $PsnT_{max}$ and $PsnT_{min}$ are maximum and minimum temperature for photosynthesis; T_{day} is daily temperature; VPD is vapor pressure deficit; $DVVPD1$ and $DVVPD2$ are fixed coefficients; $DWater$ is the index for soil moisture stress (see below).

Rate of potential transpiration is calculated as a function of potential photosynthesis (i.e., gross photosynthesis divided by $DWater$) and

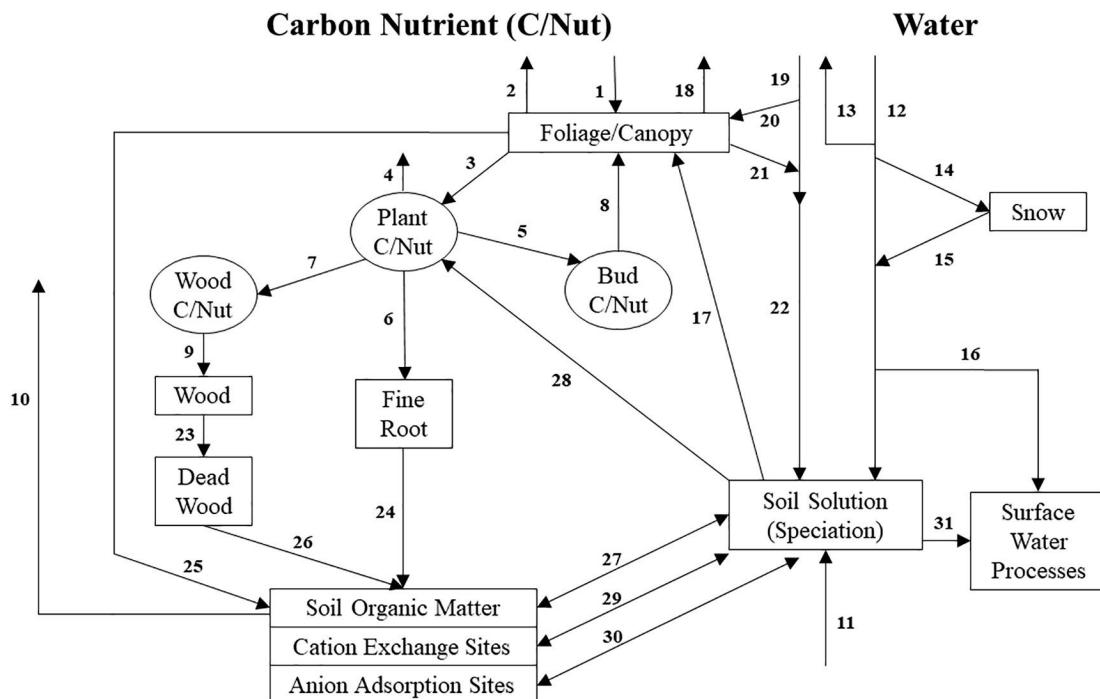


Fig. 1. PnET-BGC model structure showing depicted pools and fluxes of water, carbon, and nutrients (after Gbondo-Tugbawa et al., 2001). Processes depicted: 1. Gross photosynthesis; 2. Foliar respiration; 3. Transfer to mobile C; 4. Growth and maintenance respiration; 5. Allocation to buds; 6. Allocation to fine roots; 7. Allocation to wood; 8. Foliar production; 9. Wood production; 10. Soil respiration; 11. Weathering supply; 12. Precipitation; 13. Interception; 14. Snow-rain partition; 15. Snowmelt; 16. Shallow flow; 17. Water uptake; 18. Transpiration; 19. Deposition (wet and dry); 20. Foliar nutrient uptake; 21. Foliar exudation; 22. Throughfall & stemflow; 23. Wood litter; 24. Root litter; 25. Foliar litter; 26. Wood decay; 27. Mineralization/immobilization; 28. Nutrient uptake; 29. Cation exchange reactions; 30. Anion adsorption reactions; 31. Drainage.

water-use efficiency (WUE) which is inversely proportional to vapor pressure deficit. Actual transpiration is further limited by availability of soil moisture.

PnET-BGC considers light attenuation through the canopy and the understory, and calculates foliar display by month from gross photosynthetic rate which is affected by environmental stress from soil moisture, air temperature, and vapor pressure deficit (Aber, 1992; Aber et al., 1996). Light attenuation is calculated using the equation

$$I_i = I_0 * e^{-k*LAI_i} \quad (6)$$

where I_i is the solar radiation at canopy layer i ; I_0 is the solar radiation at the top of canopy (model input); k is the attenuation coefficient; and LAI_i is the leaf area index at canopy layer i .

Foliar display is determined by environmental conditions of the current month as well as the C balance of the previous year. To accurately simulate phenological controls on foliage development and assure a leaf acquires enough C in excess of respiration over its lifetime to repay the cost of producing that leaf, the timing of foliar expansion is regulated by the growing-degree-days, and the quantity of foliar production for a year is constrained by the average monthly foliar C balance during the growing season of the previous year (Aber, 1992). A low average monthly foliar C balance during the growing season of a year due to environmental stress may result in decreases in foliar production during the next year. Regrowth of the forest is expected in the years that follow, if the environmental stress is not repeated, as the mortality-induced canopy gaps introduce more available solar radiation to the lower canopy levels and the understory.

Wood production is calculated in the model by drawing a fraction of carbon from plant internal storage pool (PlantC) (Aber et al., 1995), which results in transport of C from the phloem to xylem. The plant internal storage carbon pool (PlantC) conceptually simulates the non-structural carbohydrates (NSC). It receives inputs of C from photosynthesis and outputs occur through different forms of respiration and allocation. Wood growth respiration is controlled by wood production; wood maintenance respiration is directly proportional to gross photosynthesis (Ryan, 1991); wood decomposition respiration is affected by the accumulation of wood litter which is related to wood biomass and production; root growth and maintenance respiration are both directly proportional to allocation of C to root biomass which is a linear function of foliar production in the model (Aber et al., 1995). NEP is calculated in PnET-BGC as the difference between total photosynthesis and the sum of all respiration terms, including growth and maintenance respiration of foliage, wood, and root, as well as wood decomposition respiration and soil microbial respiration.

Potential CO₂ fertilization effects on vegetation are simulated in PnET-BGC by a relation between plant internal CO₂ concentration and photosynthetic rate per unit leaf area using the Michaelis–Menten equation (Ollinger et al., 2009). Elevated CO₂ concentration may also increase water-use efficiency, and potentially alleviate soil moisture stress for plants and further affect foliar display (Ollinger et al., 2009). Noting that there is uncertainty over the realization of these effects, PnET-BGC can be run with or without the potential CO₂ fertilization effects.

In PnET-BGC, the rate of SOM decomposition decreases linearly with decreasing substrate content and soil moisture, and increases exponentially with temperature. Mineralization of elements from SOM including C, N, and other nutrient elements are calculated based on soil temperature, soil moisture, and SOM substrate quantity. Net mineralization of N is also a function of soil N content; higher soil N content results in a higher fraction of N immobilization. To characterize the degree of N limitation in microbial production and the competition between microbial and plant demand for N, PnET-BGC simulates a fraction of mineralized N to be immobilized, with the difference between gross N mineralization and immobilization defined as net N mineralization. The model assumes complete immobilization below 0.2% N in soil organic matter and no immobilization above 1.5% N in soil organic matter (Aber et al., 1997;

Prescott et al., 2000). A 50% resorption of N from leaves occurs before senescence. Plant uptake of N from soil solution is calculated by multiplying available N in soil solution by the ratio of plant internal N (PlantN) to the maximum storage in plant tissues (Aber et al., 1997). The concept of PlantN is similar to PlantC as it depicts the N storage in plant tissues. Computationally, uptake of NH₄⁺ and NO₃[−] increase as plant N decreases or NH₄⁺ and NO₃[−] in soil solution increases.

We used two parameters to quantify the effect of drought on photosynthesis and decomposition of soil organic matter, respectively. Plant soil moisture stress index (DWater), which is defined as the ratio between actual and potential transpiration, depicts the degree of soil moisture stress on plants. This value approaches 0 when plants are under extreme soil moisture stress and equals 1 when soil moisture stress is completely removed. Soil moisture index is defined as the ratio between soil water content and water holding capacity of the soil, and it influences the rate of SOM decomposition. A detailed description of model parameters for the old-growth Douglas-fir forest used in this study is provided in supplemental material (Table S1).

Prior to this study, vapor pressure deficit (VPD) was calculated within PnET-BGC from maximum and minimum temperature, in which air was considered saturated at minimum temperature. While this assumption is valid at some sites, it is not necessarily the case at HJA especially during dry summers. Additionally, statistical downscaling of climate data was conducted separately for maximum and minimum air temperatures, which may cause inconsistencies between calculated and observed VPD at HJA. To address these potential issues, the algorithm that calculates VPD was modified to use relative humidity (RH) as inputs.

2.3. Simulation procedures

Simulations were run from 1000 to 1850 CE with background pre-industrial estimates of meteorology, atmospheric deposition, and CO₂ concentrations to allow the model outputs to reach steady-state. We then applied linear increases while scaling the month-to-month variation to represent gradual changes in these variables until the first year of available meteorology (1958) and atmospheric deposition (1980) observations. Previous applications of PnET-BGC in the northeastern U.S. constructed emission-deposition relations to hindcast time-series inputs. This approach was not used in this study because atmospheric deposition is low at the H. J. Andrews Experimental Forest; about 10% of values observed in the eastern U.S., which is comparable to pre-industrial atmospheric deposition (Fakhraei et al., 2016). Constant future deposition at measured values was used in this study.

Projections were made from 2011 to 2100 with and without application of the algorithm of CO₂ fertilization effects on vegetation using downscaled future climate scenarios. Future CO₂ concentrations were downloaded from the RCP database for RCP4.5 (Clarke et al., 2007; Smith and Wigley, 2006; Wise et al., 2009) and 8.5 scenarios (Riahi et al., 2007). These two scenarios were selected in this study from a total of four RCP scenarios for 1) their depiction as a realistic range of future climate change; 2) the considerable relevant literature used during the initial development of RCPs (van Vuuren et al., 2011); and 3) their similarity in radiative forcing with the A2 and B1 scenarios from the Special Report on Emission Scenarios (SRES) assessed in the fourth assessment report (AR4) by the IPCC (Collins et al., 2013). Future atmospheric deposition used in this study was the average of observations from 1980 to 2010. Future RH used in this study was the average of observations from 1980 to 2010 because recent studies suggest values are unchanged (Randall et al., 2007) or decreasing RH (Sherwood et al., 2010) over most land areas by the end of the century, and any decreases in RH are expected to be small in the Pacific Northwest due to the underlying mechanism Sherwood et al. termed “last-saturation-temperature constraint” (Collins et al., 2013). We present time series of the model outputs, and compare the long-term average and interannual variability of simulations for 1986–2010 with those projected for

2076–2100. To address interannual variation of model outputs for the 2076–2100 period, we report the mean values of projections using four General Circulation Models (GCMs).

2.4. Model performance and sensitivity analysis

To validate performance of the model, simulations from 1980 to 2010 using observed climate (Daly and McKee, 2013), CO₂ concentration (Dlugokencky et al., 2016), and atmospheric deposition (NADP, 2016) inputs were compared with historical observations from Watershed 2 or simulations from other regional studies. We used two metrics, normalized mean error (NME) and normalized mean absolute error (NMAE) (Janssen and Heuberger, 1995), to evaluate performance of the model in aboveground NPP, stream water chemistry, and stream discharge,

$$NME = \frac{\bar{P} - \bar{O}}{\bar{O}} \quad (7)$$

$$NMAE = \frac{\sum_{i=1}^n (|P_i - O_i|)}{n\bar{O}} \quad (8)$$

where \bar{P} and \bar{O} are means of predicted and observed values, P_i and O_i are predicted and observed values at time i , and n is the number of observations. $NME > 0$ indicates overestimation, and a value < 0 indicates underestimation. $NMAE$ ranges from 0 to ∞ , with 0 being optimal.

We conducted a sensitivity analysis to evaluate uncertainty in the output of the deterministic model caused by inaccuracy of different model inputs (Saltelli et al., 2004). A first-order sensitivity index approach was selected for its reliability, efficiency, and relatively low computational expense (Jørgensen and Bendoricchio, 2001; Saltelli et al., 2005). This unit-independent index is defined as

$$S_{Xi}^Y = \frac{\partial Y / \partial Y}{\partial X_i / \partial X_i} \quad (9)$$

where Y is a model output of interest, X_i is a model input, ∂Y and ∂X_i are small changes in Y and X_i . A higher positive S_{Xi}^Y value indicates a greater sensitivity of a model output to a model input. A negative S_{Xi}^Y value indicates that increases in the value of a given input results in a decrease of the value of a given output (Table S4). The sensitivity analysis was conducted by examining changes in model outputs during 2006–2010 period in response to a 10% increase in an input factor. The two metrics used to evaluate model performance and the first order sensitivity index approach have been previously applied to PnET-BGC (Fakhraei et al., 2017; Pourmokhtarian et al., 2012; Valipour et al., 2018).

2.5. Climate change scenarios and downscaling at the H. J. Andrews Experimental Forest

To examine mechanisms and evaluate performance of different GCMs of climate projections under RCP scenarios, the World Climate Research Programme's Working Group on Coupled Modeling has promoted a set of coordinated climate model experiments which comprised the fifth phase of the Coupled Model Intercomparison Project (CMIP5) (Taylor et al., 2012). A recent study evaluated performance of CMIP5 models in the Pacific Northwest (Rupp et al., 2013). Four climate models in CMIP5 (CCSM4, HadGEM2-CC, MIROC5, and MRI-CGCM3) were selected for our study based on the following criteria. Selected climate models must have maximum and minimum temperature, precipitation, and solar radiation as outputs; must span the range of climate sensitivity to greenhouse gas emissions; and outputs of regional simulations may not consistently perform poorly in many regions and for many variables. The use of multiple GCMs encompasses the ability of different models to accurately project different climate outputs (e.g.

maximum temperature, minimum temperature, precipitation, solar radiation).

Simulated climate from large-scale climate models were statistically downscaled using the Asynchronous Regional Regression Model (ARRM) (Stoner et al., 2013). The ARRM downscaling technique builds a statistical relationship between daily observed meteorology at the site and historical simulated climate at the regional scale for each month during a period over 30 years using piecewise quantile regression, then applies the regression parameters to regional GCM projections to generate station-based future climate. Evaluation of the performance of ARRM downscaling method (Dixon et al., 2016) and its effects on ecological and hydrological modeling (Hay et al., 2014; Pourmokhtarian et al., 2016) have been reported in recent studies.

3. Results

3.1. Model performance and sensitivity analysis

Simulations of aboveground net primary production (NPP) for Watershed 2 at HJA from 1970 to 2010 ($416 \pm 29 \text{ g C m}^{-2} \text{ yr}^{-1}$) were comparable with observations from four previous studies with mean values ranging from 358 to $455 \text{ g C m}^{-2} \text{ yr}^{-1}$ and standard deviations ranging from 60 to $120 \text{ g C m}^{-2} \text{ yr}^{-1}$ and observations from 60 permanent plots (0.1 ha) in Watershed 2 (Shaw and Franklin, 2017) ($\text{NME} = -0.034$, $\text{NMAE} = 0.047$; Fig. S1; Table S2). Year-to-year variation in aboveground NPP is generally captured by the model except for the year 2000. The higher observed value in 2000 than other years is attributed to an overestimation of tree mortality (Pabst, personal communication). Simulations of monthly stream discharge from 1973 to 2008 were similar to observations at Watershed 2 ($\text{NME} = 0.035$, $\text{NMAE} = 0.092$; Fig. S2; Table S2). Measurements of soil moisture were primarily conducted for the upper 30 cm in Watershed 2, while measurements of soil moisture at deeper horizons are only available at HJA climate stations with open canopy and much shallower rooting depth, which limit meaningful comparison with model simulations for the entire rooting zone of the old-growth forest. However, simulated monthly transpiration was comparable with observations at Watershed 2 using sap flow sensors (Moore et al., 2004) and observations from an old-growth Douglas-fir forest in Washington using eddy-covariance (Unsworth et al., 2004; Wharton et al., 2009). Note that the old-growth forest at Watershed 2 is characterized by a much lower rate of transpiration ($< 6 \text{ cm month}^{-1}$ in summer) than the young and mature forests (Moore et al., 2004; Warren et al., 2005). Simulated transpiration showed a seasonal pattern consistent with observations from the nearby old-growth Douglas-fir forest using eddy-covariance and simulations thereof using ED2 model (Jiang et al., 2018). To validate model simulations of seasonal photosynthesis without direct observations at Watershed 2 in HJA, we compared plant internal C storage simulated by PnET-BGC (Fig. S3) with measurements of non-structural carbohydrates (NSC) concentrations in a Douglas-fir forest in southwestern Washington State (Woodruff and Meinzer, 2011). The magnitude and seasonal pattern of simulated NSC concentrations of total biomass in 1986–2010 was comparable with measured NSC concentrations in the trunk and branch of tall (56.5 m) Douglas-fir trees in 2009 and 2010 (see Figs. 1 and 3 a in Woodruff and Meinzer, 2011). Both simulations and observations were characterized by increasing trends in winter and spring as the photosynthate accumulates and decreasing trends in summer after the bud swell and leaf expansion.

Model simulations of stream water chemistry were similar to long-term average observations from 1981 to 2009, but did not capture year-to-year variations for some elements (Table S2). Model simulations were less accurate for SO₄²⁻, NH₄⁺, and NO₃⁻ but note that these solutes exhibit low stream water concentrations. Long-term average simulated values for major biogeochemical pools/fluxes were comparable with or in the range of observations and simulations reported by previous studies (Table S3). Model performance of PnET-BGC for HJA

was comparable with simulations for the Hubbard Brook Experimental Forest in New Hampshire (Pourmokhtarian et al., 2012) and simulations for HJA using another biogeochemical model (Hartman et al., 2009).

Sensitivity analysis shows that model simulations of major C pools and fluxes are generally more responsive to certain parameters including the slope of relationship between leaf N and max photosynthetic rate (AmaxB), respiration as a fraction of maximum photosynthesis (BFolResp), minimum N fraction in foliar litter (FLPctN), foliage retention time (FolRet), half saturation light level (HalfSat), light attenuation constant (k), optimum temperature for photosynthesis (PsnTOpt), specific leaf weight (SLWmax), and meteorological inputs including photosynthetically active radiation (PAR) and air temperature (Tmax and Tmin) (Table S4 a). Model simulations of transpiration and soil moisture index are also responsive to most of the above-mentioned factors, but simulations of stream discharge are much more responsive to precipitation (Prec) and the fraction of precipitation intercepted and evaporated (PrecIntFrac) than other factors (Table S4 b). Sensitivity analysis indicates that model simulations of N dynamics are highly responsive to input factors that affect C and water pools and fluxes. Simulations of the N content of SOM and net N mineralization are also responsive to decomposition constant for SOM pool (ksom), minimum N fraction in root litter (RLPctN), and slope of relationship between leaf and root allocation (RootAIB) (Table S4 c). This sensitivity analysis suggests that uncertainty in the above-mentioned input factors are likely major contributors to uncertainty in model outputs. To reduce the uncertainty in simulations of water, C, and N dynamics at Watershed 2 in HJA, improvements on measurement accuracy in these model inputs are needed.

3.2. Downscaled future climate change scenarios

Downscaled climate projections showed that annual mean temperature is expected to increase by 2.4 to 7.1 °C from 1986–2010 to 2076–2100 for Watershed 2 at HJA (Fig. S4). Monthly projections showed larger increases in temperature in August and September than in other months under both RCP4.5 and RCP8.5 scenarios, resulting in a shift of the warmest month of a year from July to August (Fig. 2 a). Annual precipitation is projected to slightly change ranging from −19.9 to 13.6 cm from 1986–2010 to 2076–2100 (Fig. S5). Note that projected changes in annual precipitation for HJA are small relative to its magnitude and annual variation. No distinctive pattern in precipitation was found among projections by different GCMs.

3.3. Water cycling under climate change scenarios

Projections of transpiration at ecosystem level show different patterns from that of leaf stomatal conductance at Watershed 2. Transpiration per unit of land area is projected to decrease from 15.8 (long-term average) ± 2.0 (interannual variability) cm yr^{-1} in 1986–2010 to 12.8 (long-term average) ± 1.1 (mean interannual variability of projections using inputs from four GCMs) cm yr^{-1} ($11.3 \pm 1.0 \text{ cm yr}^{-1}$ with CO_2 effects) in 2076–2100 under the RCP4.5 scenario, and $4.6 \pm 2.5 \text{ cm yr}^{-1}$ ($3.9 \pm 2.5 \text{ cm yr}^{-1}$ with CO_2 effects) under the RCP8.5 scenario (Fig. 3). Stomatal conductance (per unit of leaf area) is projected to increase throughout the year from 1986–2010 to 2076–2100 under both the RCP4.5 and RCP8.5 scenarios (Fig. 2 b) despite the projected reduction in leaf C assimilation in July and August (see below). In 2076–2100, stomatal conductance is projected to be higher without CO_2 effects than with CO_2 effects. In contrast to the pattern in ecosystem-level transpiration, stomatal conductance is projected to be substantially higher under the RCP8.5 than the RCP4.5 scenario, except for July and August. Projected decreases in transpiration per unit of land area coupled with nearly constant future seasonal precipitation leads to anticipated increases in soil moisture in summer and fall especially under the high radiative forcing scenario (Fig. 4). As a result, vegetation at Watershed 2 is not expected to experience chronic soil moisture stress in the future

(Fig. 5 a b). The magnitude of change in annual transpiration is small relative to precipitation, therefore projected annual stream discharge is primarily driven by future precipitation ($R^2 = 0.91$). However, summer discharge is projected to increase from $2.6 \pm 2.5 \text{ cm yr}^{-1}$ in 1986–2010 to $5.5 \pm 4.8 \text{ cm yr}^{-1}$ ($5.8 \pm 4.9 \text{ cm yr}^{-1}$ with CO_2 effects) in 2076–2100 under the RCP8.5 scenario corresponding to the large decreases in transpiration per unit of land area.

3.4. Carbon cycling under climate change scenarios

Projections with and without potential CO_2 fertilization effects show long-term decreases in future foliar NPP at Watershed 2 in HJA regardless of the GCM simulation considered (Fig. 6 a b). Average foliar NPP is projected to decrease from $104.5 \pm 6.3 \text{ g C m}^{-2} \text{ yr}^{-1}$ in 1986–2010 to $55.2 \pm 7.1 \text{ g C m}^{-2} \text{ yr}^{-1}$ and $15.1 \pm 12.4 \text{ g C m}^{-2} \text{ yr}^{-1}$ in 2076–2100 under the RCP4.5 and RCP8.5 scenarios, respectively. Monthly projections show large declines in foliar biomass from 1986–2010 to 2076–2100 under both scenarios corresponding to the decreasing foliar NPP (Fig. 2 a). Projections of monthly foliar biomass also show an advanced start of leaf expansion in spring. Leaf C assimilation (net photosynthesis per unit of leaf area) is projected to increase substantially from 1986–2010 to 2076–2100 between October and June (Fig. 2 c). However, the rate is projected to decrease drastically in July (RCP8.5) and August (RCP4.5 and RCP8.5), with little change in September. In 2076–2100, net photosynthesis per unit of leaf area under the RCP8.5 scenario is projected to be higher than the RCP4.5 scenario from October to May, but lower than the RCP4.5 scenario from June to September. Projections considering potential CO_2 fertilization effects result in higher leaf C assimilation than projections without CO_2 effects in all months in 2076–2100, except for December in which the rates are projected to be negative. Net photosynthetic rate per unit of ground area is projected to markedly decrease from $858 \pm 45 \text{ g C m}^{-2} \text{ yr}^{-1}$ in 1986–2010 to $584 \pm 56 \text{ g C m}^{-2} \text{ yr}^{-1}$ and $196 \pm 106 \text{ g C m}^{-2} \text{ yr}^{-1}$ in 2076–2100 under the low and high radiative forcing scenario, respectively. Model simulations also demonstrate that although photosynthetic rate per unit of ground area is expected to be higher with potential CO_2 fertilization effects on vegetation ($691 \pm 65 \text{ g C m}^{-2} \text{ yr}^{-1}$ under RCP4.5 and $242 \pm 130 \text{ g C m}^{-2} \text{ yr}^{-1}$ under RCP8.5 in 2076–2100), there is no difference in future foliar NPP or foliar biomass when potential CO_2 fertilization effects were considered.

We also observed strong relationships ($R^2 = 0.80$, $p < 0.001$) between foliar NPP and the previous-year temperature projected from different radiative forcing scenarios with the GCMs. Simulations of foliar NPP for a year are strongly controlled by the mean temperature of the warmest month in the previous year (Fig. 7). Under future climate, each degree Celsius increase in the temperature of the warmest month in a year from 19.9 °C (the average temperature of the warmest month in a year for 1986–2010) is projected to lead to a decrease in foliar production in the next year by $11.1 \text{ g C m}^{-2} \text{ yr}^{-1}$.

Projections of future wood production without potential CO_2 fertilization effects show little long-term change before the 2050s under the RCP4.5 and RCP8.5 scenarios (Fig. 6 c d). Under the RCP4.5 scenario, wood NPP is projected to decrease from $323 \pm 18 \text{ g C m}^{-2} \text{ yr}^{-1}$ in 1986–2010 to $278 \pm 19 \text{ g C m}^{-2} \text{ yr}^{-1}$ in 2076–2100. Under the RCP8.5 scenario, wood production at Watershed 2 is projected to substantially decrease to $122 \pm 52 \text{ g C m}^{-2} \text{ yr}^{-1}$ in 2076–2100. Effects of potential CO_2 fertilization were more evident on wood NPP than foliar NPP. Under the RCP4.5 scenario, projections with potential CO_2 fertilization effects show increases in wood NPP until the 2050s and then slightly decrease to $355 \pm 21 \text{ g C m}^{-2} \text{ yr}^{-1}$ in 2076–2100. The RCP8.5 scenario with potential CO_2 fertilization effects also results in higher wood NPP of $162 \pm 56 \text{ g C m}^{-2} \text{ yr}^{-1}$ in 2076–2100 compared with simulations without CO_2 effects. Net ecosystem production (NEP) is projected to decrease to $-39 \pm 52 \text{ g C m}^{-2} \text{ yr}^{-1}$ in 2076–2100 under the RCP4.5 scenario without CO_2 fertilization (Fig. 6 e). Under the high radiative forcing scenario, NEP is projected to markedly decrease from

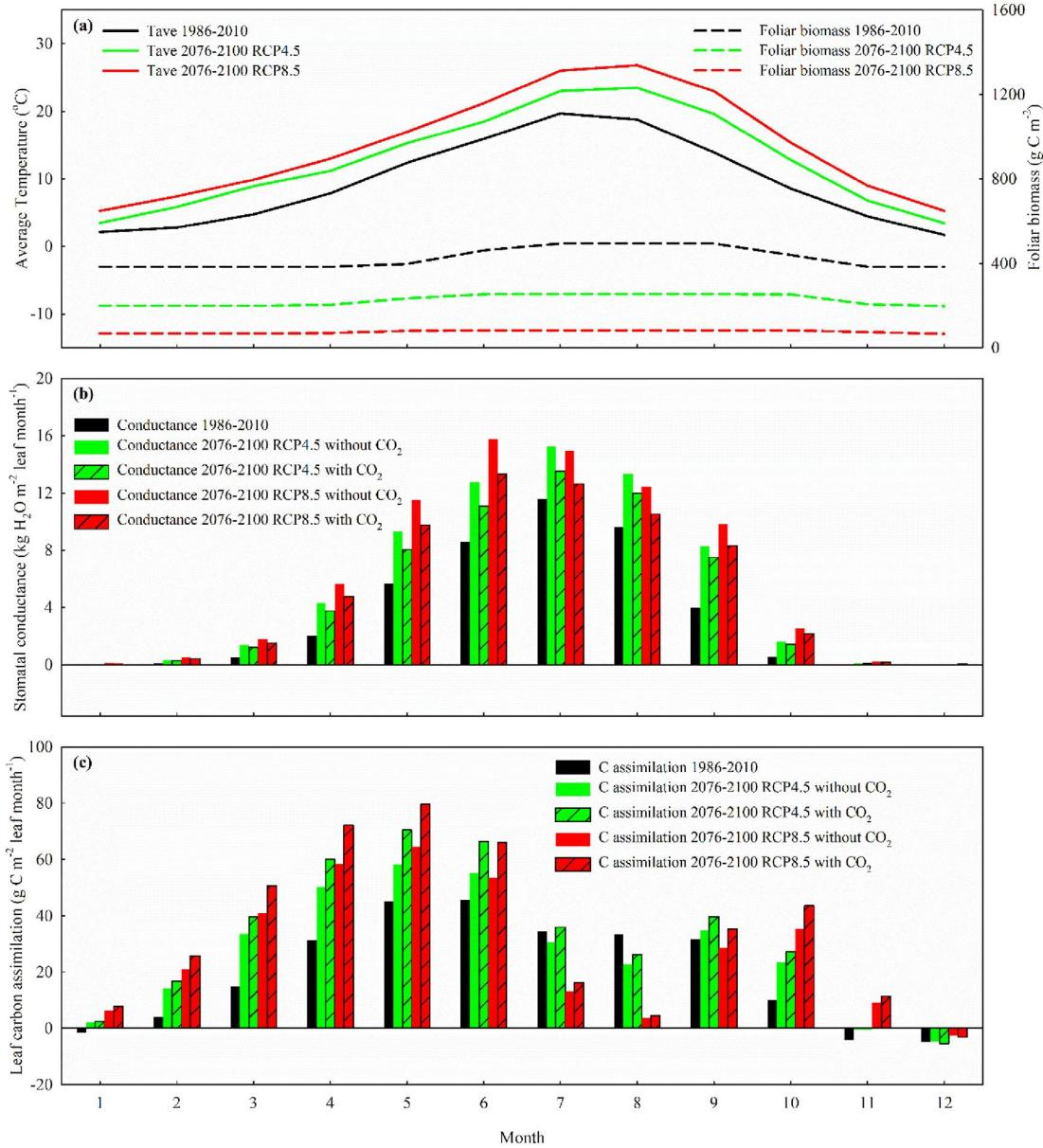


Fig. 2. Past simulations (1986–2010) and future projections (2076–2100) of monthly average temperature and foliar biomass (a), stomatal conductance (b), and leaf carbon assimilation (c) under the RCP4.5 and RCP8.5 scenarios for Watershed 2 at the H. J. Andrews Experimental Forest. Projections shown are the average using climate inputs from four GCMs for each scenario.

$48 \pm 61 \text{ g C m}^{-2} \text{ yr}^{-1}$ ($106 \pm 64 \text{ g C m}^{-2} \text{ yr}^{-1}$ with potential CO₂ fertilization effects) in the 2030s to $-303 \pm 24 \text{ g C m}^{-2} \text{ yr}^{-1}$ in the 2090s ($-294 \pm 25 \text{ g C m}^{-2} \text{ yr}^{-1}$ with potential CO₂ fertilization effects) (Fig. 6f).

Projected changes in foliar and wood production in the upcoming decades may be expected to cause corresponding changes in foliar and wood litter. Model projections showed future decreases in total litter calculated as the sum of foliar, wood, and root litter under both the RCP4.5 and RCP8.5 scenarios (Fig. 8). Considering potential CO₂ fertilization effects in the model results in negligible difference in total litter from model runs which excluded CO₂ effects on vegetation. By the 2090s, the difference in projected total litter is below $3 \text{ g C m}^{-2} \text{ yr}^{-1}$ with and without considering potential CO₂ fertilization effects.

Decomposition of SOM is projected to change little from historical simulated value ($251 \pm 16 \text{ g C m}^{-2} \text{ yr}^{-1}$ from 1986 to 2010) over the near-term, then start to decrease from the early 2030s or 2050s until the end of the century to levels below the current SOM content

depending on the future climate change scenario considered (Fig. 8). Future decomposition of SOM is projected to have negligible difference if potential CO₂ fertilization effects on vegetation are considered. Projected total litter is expected to decrease to values less than decomposition of SOM regardless of the climate change scenario considered. As a result, the SOM pool is projected to decrease from the historical simulated value of $10,563 \pm 18 \text{ g C m}^{-2}$ (from 1986 to 2010) to $6061 \pm 425 \text{ g C m}^{-2}$ and $4014 \pm 781 \text{ g C m}^{-2}$ in 2076–2100 under the RCP4.5 and RCP8.5 scenarios, respectively. Note that net loss of SOM under the RCP8.5 scenario is projected to exceed $100 \text{ g C m}^{-2} \text{ yr}^{-1}$ after the 2070s. We illustrate the C mass balance for each decade in the past and future under climate change scenarios to demonstrate relative changes in carbon pools and fluxes in Appendix S1.

3.5. Nitrogen cycling under climate change scenarios

Although projections show contrasting future trends of C storage in live plant biomass under the RCP4.5 and RCP8.5 scenarios (Fig. S6),

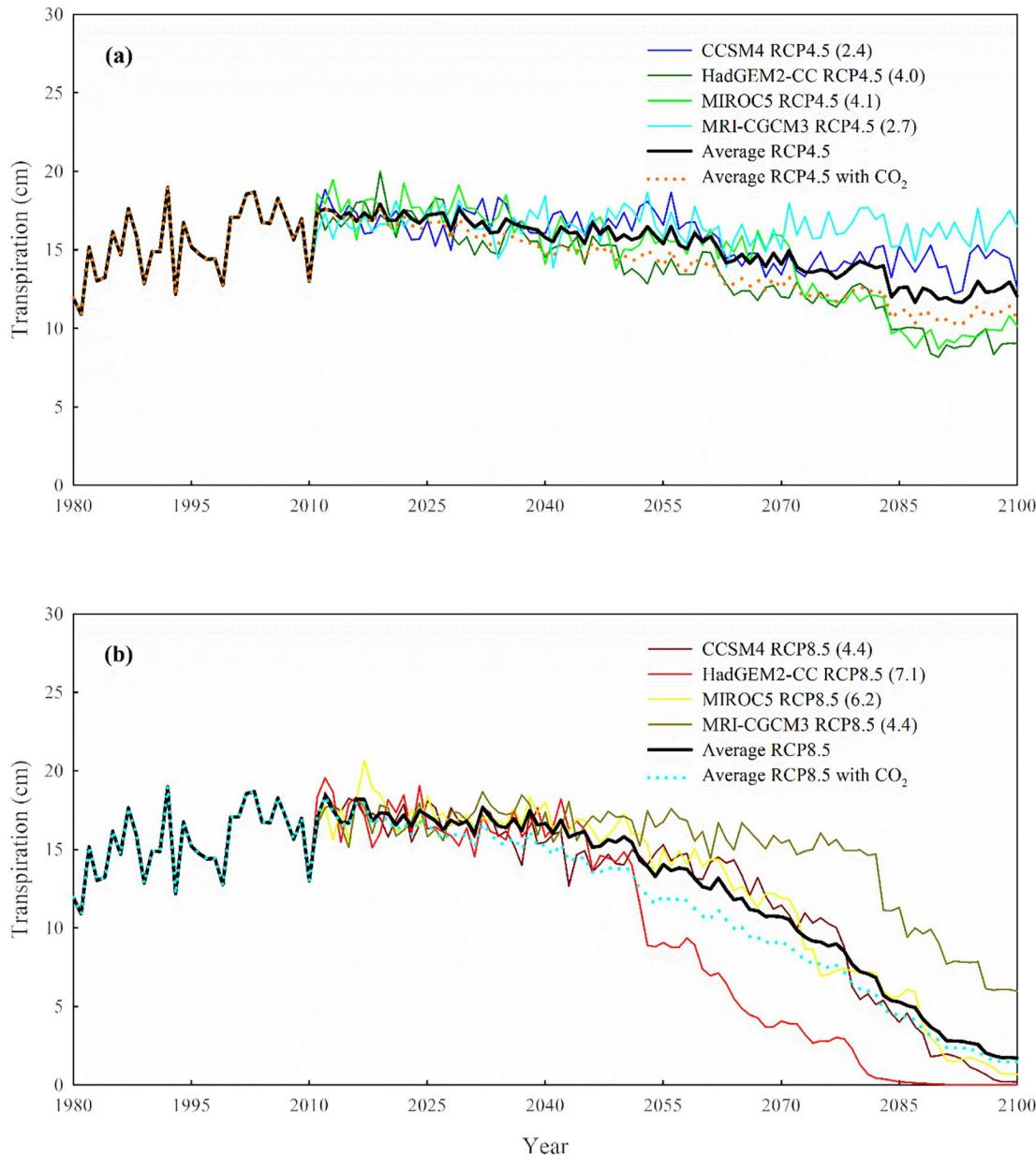


Fig. 3. Past simulations (1980–2010) and future projections (2011–2100) of transpiration under the RCP4.5 (a) and RCP8.5 (b) scenarios for Watershed 2 at the H. J. Andrews Experimental Forest. Projections shown used climate inputs from four GCMs. The values in parentheses for GCM labels indicate increases in annual mean temperature ($^{\circ}\text{C}$) from 1986–2010 to 2076–2100.

foliar N concentration is projected to increase slightly in the 21st century under both climate change scenarios (Fig. S7). The percentage of N in foliage of 1.24% is projected to increase to 1.25% and 1.26% by the end of the century under RCP4.5 and RCP8.5, respectively. Projections with and without potential CO_2 fertilization effects show negligible differences in foliar N concentration (Fig. S7). The N content (in g N m^{-2}) in SOM is projected to decrease with soil organic carbon (SOC) throughout the simulation period under both low and high radiative forcing scenarios (Fig. 8, Fig. 9). Nitrogen concentrations (percentage) in SOM, however, show contrasting patterns under future climate change scenarios. Under the RCP4.5 scenario, the N concentration in SOM is projected to increase from historical simulated value of 1.04% (from 1986 to 2010) until the 2040s to 2060s then remain at 1.06% to 1.11% by the end of the century depending on the GCM selected. Under the RCP8.5 scenario, N concentration in SOM is projected to increase to 1.14% to 1.17% depending on the GCM considered. For the warmest scenario under HadGEM2-CC, the N concentration in SOM is projected to

increase to 1.20% in the 2080s and then decrease to 1.15%. Projections with and without potential CO_2 fertilization effects on vegetation show negligible differences in N concentration in SOM (Fig. 9). PnET-BGC calculates net N mineralization as the difference between gross mineralization and immobilization. Under the RCP8.5 scenario, net N mineralization is projected to gradually increase until the 2070s then decrease (Fig. S8 b) at a lower rate than the reduction in SOM decomposition (Fig. 8 b). Stream leaching of NH_4^+ under the RCP8.5 scenario is projected to slightly increase with net N mineralization until the 2070s (Fig. S8 d). Stream leaching of NO_3^- , which historically is occasionally below the limit of detection ($0.07 \mu\text{mol/L}$) in Watershed 2, is also projected to increase under the high radiative forcing scenarios (Fig. S8 f). Invoking potential CO_2 fertilization effects on vegetation has negligible effects on projections of inorganic N in stream water at Watershed 2 in HJA. Note that the absolute concentrations of N are very low compared with forested watersheds experiencing elevated leaching losses of N (Aber et al., 2003).

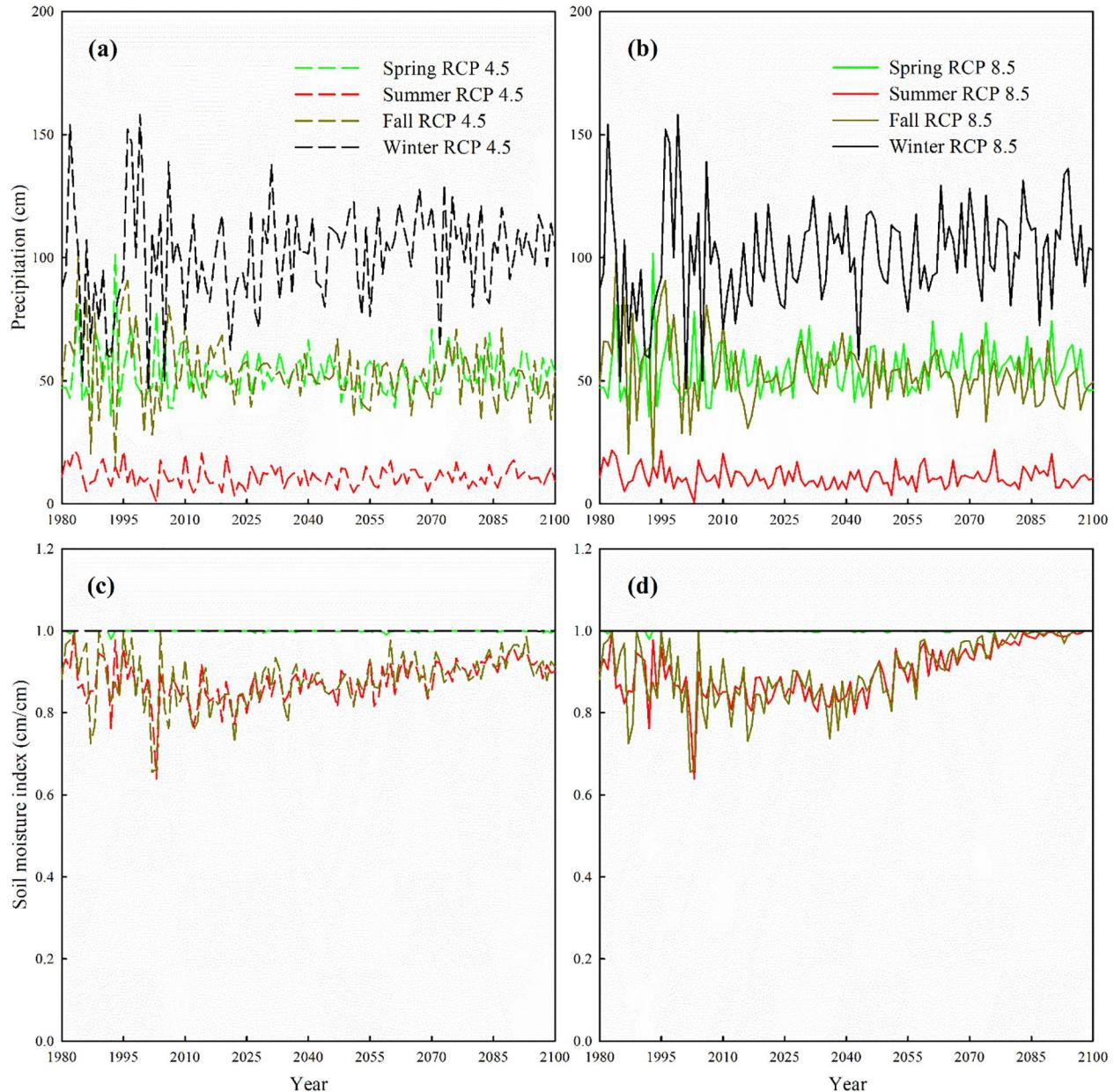


Fig. 4. Observations/past simulations (1980–2010) and future projections (2011–2100) of seasonal precipitation (a, b) and soil moisture index (c, d) under the RCP4.5 (a, c) and RCP8.5 (b, d) scenarios for Watershed 2 at the H.J. Andrews Experimental Forest. Results shown are average of projections using four GCMs without CO₂ fertilization effects on vegetation. Spring (MAM), Summer (JJA), Fall (SON), Winter (DJF).

4. Discussion

4.1. Increasing temperature as a driving factor of future changes in carbon pools and fluxes

Projected increases in leaf C assimilation corresponding to the increasing temperature from 1986–2010 to 2076–2100 for the months of October to June are attributed to the closer-to-optimal temperature for photosynthesis which facilitates carboxylation efficiency of Rubisco, and are consistent with observations from warming experiments for Douglas-fir seedlings (Lewis et al., 2001; Ormrod et al., 1999). However, our projections suggest future changes in C dynamics at Watershed 2 in HJA are likely driven by direct temperature stress (Fig. 5 c d) and heat-induced air humidity stress (Fig. 5 e f) which reduce foliar production and biomass. Although it is widely recognized that water limitation affects, and will continue to affect, C dynamics in young and mature forests in the Pacific Northwest (Berner and Law, 2015; Griesbauer and

Green, 2010a; Kang et al., 2014; Littell et al., 2010; Littell et al., 2008; Spittlehouse, 2003), future summer drought under the RCP4.5 and RCP8.5 scenarios is not projected to be severe enough to cause soil moisture stress on the old-growth Douglas-fir forest due to the reduced foliar biomass and transpiration (see discussion below).

Photosynthetic rates fall as temperature increases above an optimum due to the impairment of foliar protein function. However, it has long been speculated that acclimation can shift temperature optima (Berry and Bjorkman, 1980). PnET-BGC uses a quadratic relationship between temperature and photosynthetic rate to quantitatively represent this acclimation observed from warming and steady-state experiments (Battaglia et al., 1996; Lewis et al., 2001; Saxe et al., 2001), by which 80% of photosynthetic capacity is reached at 9 °C above the temperature optima. However, projected future marked increases in temperature at HJA (Fig. S4), especially in summer, and associated increases in vapor pressure deficit result in a low rate of photosynthesis, which explains the decreases in leaf C assimilation from 1986–2010 to

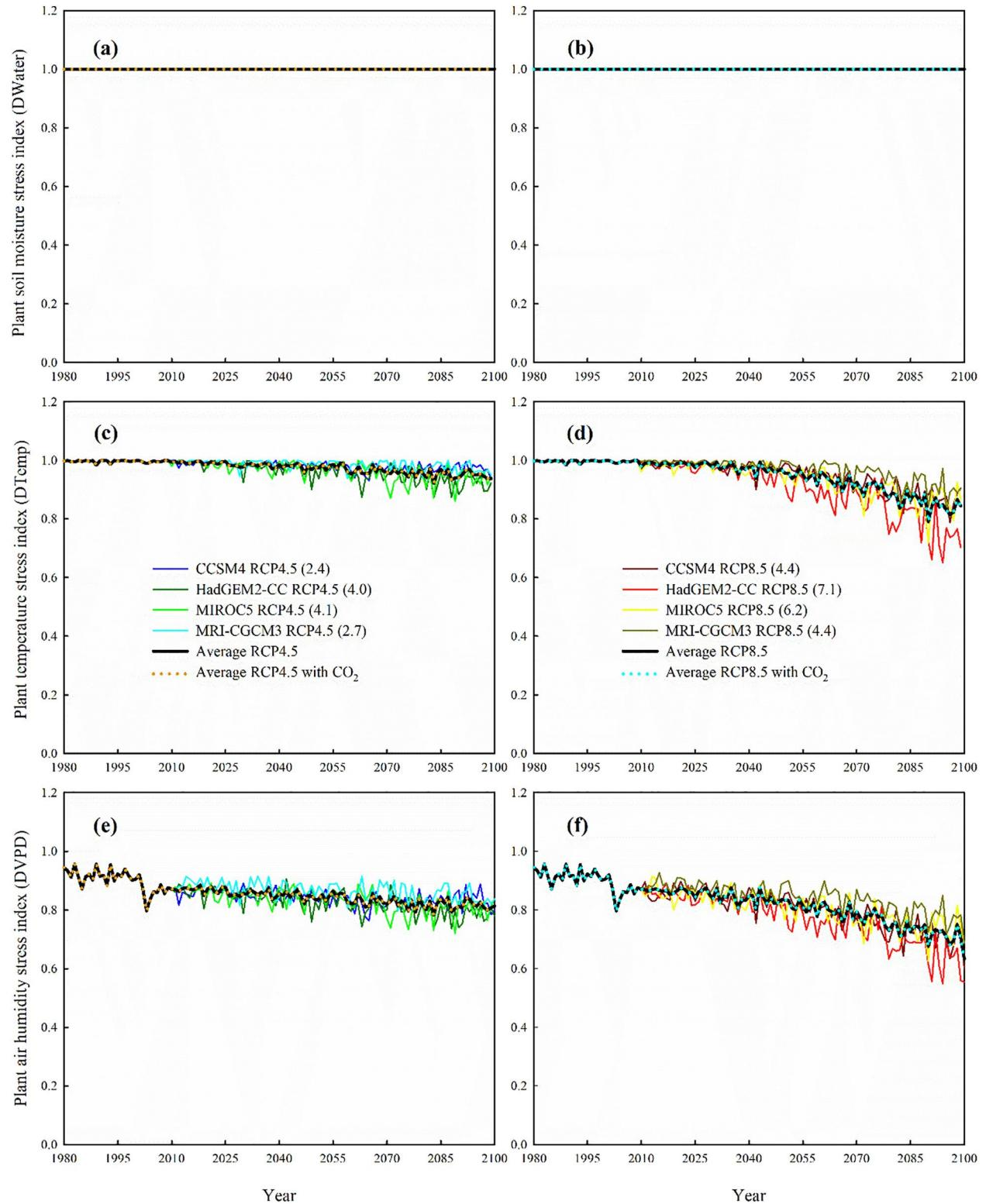


Fig. 5. Past simulations (1980–2010) and future projections (2011–2100) of plant soil moisture stress index (a, b), plant temperature stress index (c, d), and plant air humidity stress index (e, f) under the RCP4.5 (a, c, e) and RCP8.5 (b, d, f) scenarios for Watershed 2 at the H.J. Andrews Experimental Forest. Projections shown used climate inputs from four GCMs. The values in parentheses for GCM labels indicate increases in annual mean temperature ($^{\circ}\text{C}$) from 1986–2010 to 2076–2100.

2076–2100 in July through September. A reduction of leaf C assimilation in summer may decrease the average monthly leaf C balance during the growing season in the current year, and result in decreases in the foliar production and biomass in the next year. Although the mortality-induced canopy gap introduces more available solar radiation to the lower canopy levels and the understory, continuous increases in future

temperature under the RCP8.5 scenario is projected to cause repeated physiological stress which hampers regrowth of the forest in the following years.

Projections without potential CO_2 effects suggest that future net photosynthesis per unit of land area at Watershed 2 is largely driven by the decreases in foliar biomass despite increasing leaf C assimilation

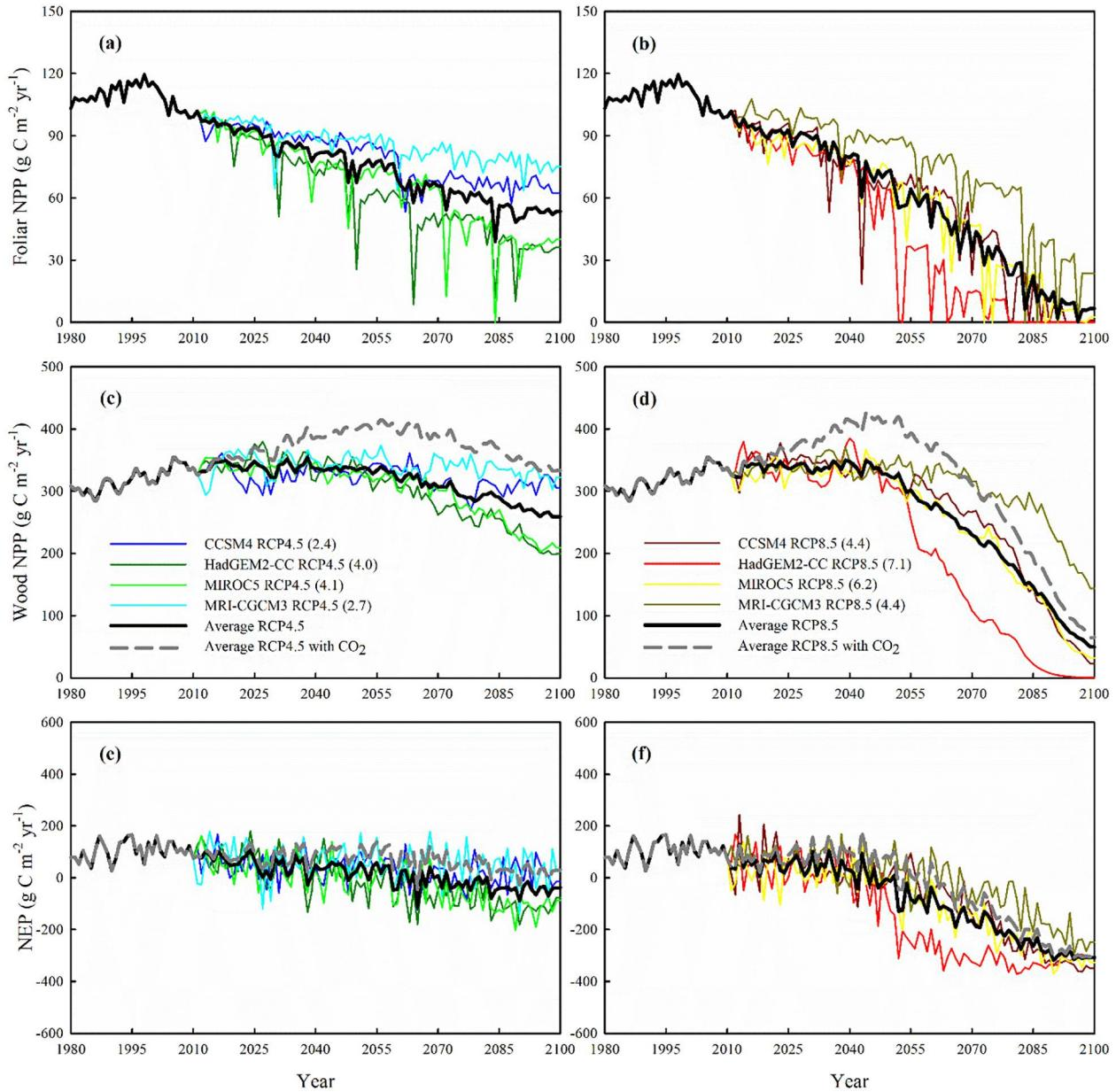


Fig. 6. Past simulations (1980–2010) and future projections (2011–2100) of foliar NPP (a, b), wood NPP (c, d), and NEP (e, f) under the RCP4.5 (a, c, e) and RCP8.5 (b, d, f) scenarios for Watershed 2 at the H. J. Andrews Experimental Forest. Projections shown used climate inputs from four GCMs. The values in parentheses for GCM labels indicate increases in annual mean temperature (°C) from 1986–2010 to 2076–2100.

from late fall to spring. Results from warming experiments have shown that increasing temperature causes decreases in summer photosynthetic rates (Lewis et al., 1999) and foliar production (Olszyk et al., 1998) in Douglas-fir forests. A recent study of seasonal patterns of temperature and foliar production at five mature Douglas-fir forests in the Pacific Northwest revealed adverse effects of temperature on foliar display above an optimum of 20 °C (Breedlow et al., 2013). In a review of data from 63 studies, Way and Oren (2010) found decreases in foliar biomass with increasing temperature above the optimum for evergreen species. Although projected increases in vapor pressure deficit are expected to decrease water-use efficiency and increase stomatal conductance, which is supported by a warming experiment for Douglas-fir seedlings (Lewis et al., 2002), reduced foliar display largely drives the simulated pattern of future transpiration at Watershed 2.

Effects of soil moisture on vegetation are quantified in PnET-BGC by the ratio of actual and potential rates of transpiration. Little change in future precipitation (Fig. 4 a b) coupled with the decreasing transpiration

(Fig. 3) is likely to increase soil moisture (Fig. 4 c d) in the old-growth forest. The moderate water holding capacity of soils at Watershed 2 (Dyrness, 1969) is projected to keep soil moisture above the demand of water by vegetation (Fig. 5 a b) through the dry summers that are projected for the future (Fig. 4 a b). Projected air temperature and humidity stress under the RCP8.5 scenarios are more detrimental to foliar production in HJA than projected soil moisture stress in several hardwood forests in the northeastern U.S. (Pourmokhtarian, 2013). We attribute this difference to the nature of soil moisture stress under which plants adjust the foliar display downward to reduce future demand for transpiration alleviating further soil moisture stress. Although current knowledge of acclimation of optimal temperature for photosynthesis is quantitatively represented in PnET-BGC, continuously increasing temperature and repeated stress under the RCP scenarios result in continuous reduction in foliar NPP and foliar biomass.

Future trends in wood production reflect projected changes in the plant internal storage C pool under climate change scenarios. Hartman

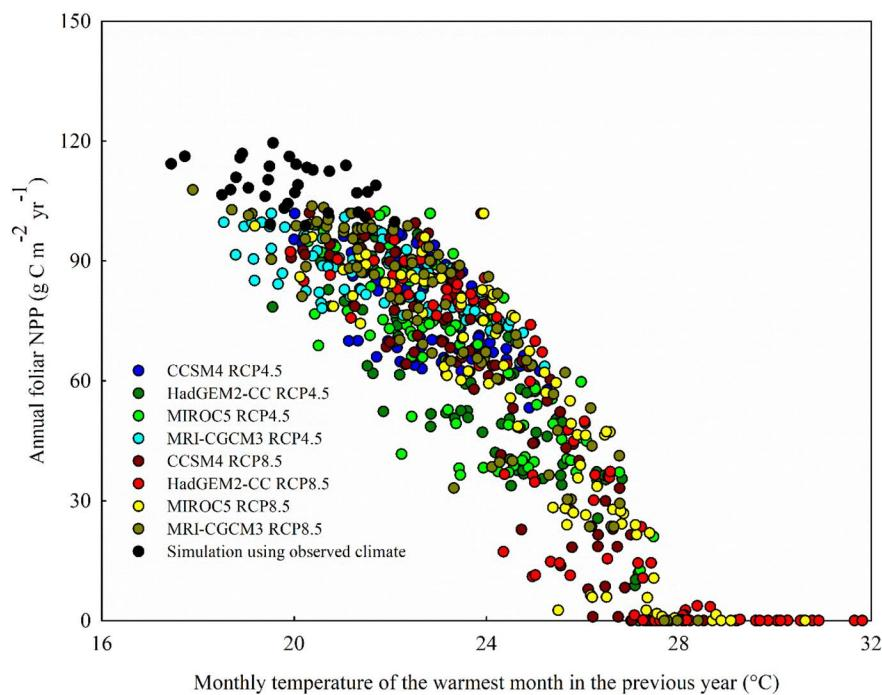


Fig. 7. Relation of annual foliar NPP with monthly temperature of the warmest month in the previous year under the RCP4.5 and RCP8.5 scenarios for Watershed 2 at the H. J. Andrews Experimental Forest. Color symbols indicate projections using future climate input from four GCMs from 2011 to 2100; black symbols indicate simulations using observed climate inputs from 1980 to 2010.

et al. (2014) projected lower future above and below ground C pools under warmer climate scenarios in both young and old-growth forests at HJA, but attributed this response to lower soil moisture rather than direct air temperature and humidity stress on photosynthesis. However, their projection of a much lower above ground C pool in the young forest of the future than old-growth forest demonstrates the importance of stand age in the response of productivity to a future warmer climate at HJA. Essentially all the respiration terms used to calculate NEP are subjected to change with increasing temperature. A mesocosm experiment conducted with young Douglas-fir showed increases in gross photosynthesis and ecosystem respiration in response to elevated temperature (Tingey et al., 2007). Projected NEP in our study agrees with the results of Tingey et al. (2007) that elevated temperature may lead to decreases in NEP.

The effect of elevated temperature on NPP is manifested through a decrease in total litter. The lack of change in SOM decomposition in the near-term with relatively small change in substrate quantity is consistent with observations from a soil warming experiment using Douglas-fir seedlings grown in reconstructed litter-soil systems (Tingey et al., 2006). Litter serves as an input of SOM. Its continuous decrease accelerates loss of SOM over the long-term as SOM decomposition continues. Though the combined effects of increases in temperature and decreases in litter inputs under nearly constant soil moisture until the early 2030s or 2050s under RCP4.5 or RCP8.5, respectively, SOM is able to maintain nearly constant rates of decomposition. However, after the 2030s or 2050s, depending on the climate change scenario considered, a much lower amount of litter input overcomes the effects of higher temperature and soil moisture resulting in lower rates of decomposition. Our projections are consistent with findings of supply-side controls on SOM decomposition (Campbell et al., 2004), and agree with Hartman et al. (2014) that SOC decreases in the future. However, PnET-BGC does not consider effects of litter quality on soil heterotrophic respiration. Hartman et al. (2014) also projected slower increases in heterotrophic respiration under warmer scenarios at HJA, which is consistent with our projections that SOM decomposition is lower under the RCP8.5 than RCP4.5 scenario. However, our simulations suggested that

lower SOM decomposition projected under the high radiative forcing scenario was due to lower productivity and substrate content, rather than lower soil moisture.

4.2. Effects of allocation and immobilization on future nitrogen dynamics

Projected decreases in N allocation to foliage coupled with little change in plant uptake of N result in an increase in accumulation of N in plant tissues. This future increase in accumulation of plant N results in increases in foliar N concentrations and subsequent increases in N concentrations in SOM. Decrease in N concentration in SOM after the 2080s for the RCP8.5 scenario under HadGEM2-CC results from low foliar NPP and the dominance of total litter by wood litter which has very low N concentration. The prescribed relationship in PnET-BGC (Table S1) suggests that projected increases in foliar N concentration only have a minor contribution to leaf C assimilation (<3% increase). Projected changes in net N mineralization may not be solely attributed to changes in decomposition of SOM especially by the end of the century. Projected increases in N concentration of SOM from 1.04% (1986–2010) to 1.08% (2076–2100 under RCP4.5) or 1.16% (2076–2100 under RCP8.5) alters the immobilization of N from 38% (1986–2010) to 35% (2076–2100 under RCP4.5) or 29% (2076–2100 under RCP8.5). The projected gradual increases in net N mineralization until the 2070s under the RCP8.5 scenario result from increases in concentrations of N in SOM and a decreasing percentage of N immobilization. This relation of net N mineralization with soil N stoichiometry is consistent with observations by Perakis and Sinkhorn (2011) from nine Douglas-fir forests in the north-central Oregon Coast Range and observations by Prescott et al. (2000) from nine Douglas-fir forests in Oregon and Washington.

Our projections assume future atmospheric deposition of NH_4^+ and NO_3^- remain constant and are equivalent to the average of observations from 1980 to 2010. Gradually increasing net N mineralization until the 2070s under the RCP8.5 scenario leads to slow increases in NH_4^+ in soil solution and stream water because accumulation of N in plant tissues slightly decreases the fraction of NH_4^+

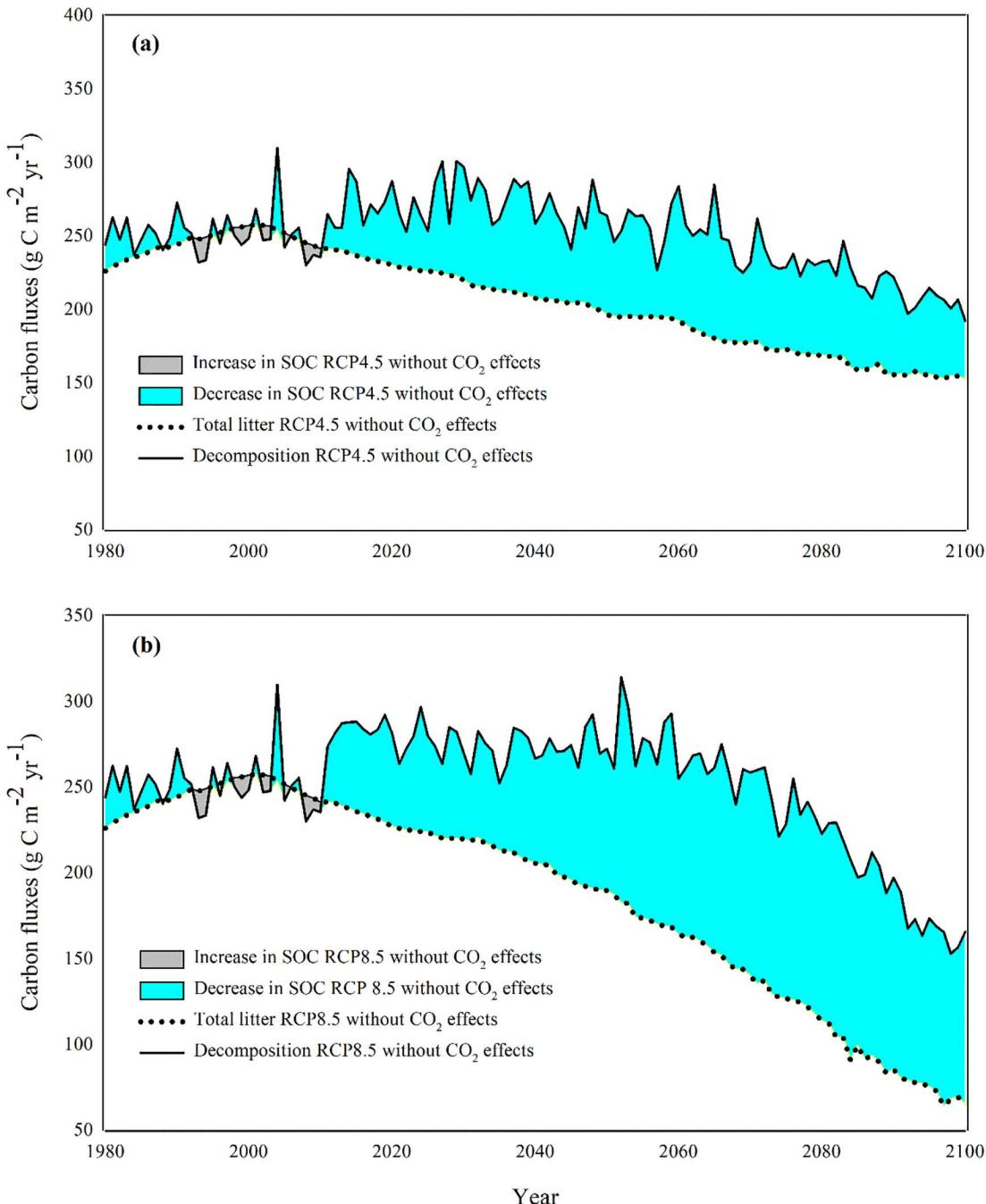


Fig. 8. Historical simulations (1980–2010) and future projections (2011–2100) of total litter and SOM decomposition under the RCP4.5 (a) and RCP8.5 (b) scenarios for Watershed 2 at the H. J. Andrews Experimental Forest. Results shown are the average of projections using climate inputs from four GCMs for each scenario without CO₂ fertilization effects on vegetation.

uptake from soil solution. Since our projections suggest net nitrification will continue to be low at HJA under future climate, projected increases in NO₃[−] concentration of stream water is the result of slight decreases in plant uptake of NO₃[−] associated with the accumulation of N in plant tissue. Plant uptake currently draws over 99% of inorganic N from soil solution at HJA, and this retention is projected to remain high (>98%) even under the warmest climate change scenario. The high efficiency of plant uptake minimizes loss of N from the ecosystem. A modeling study in the western U.S. suggested an alleviation of N-limiting conditions due to increasing soil moisture and mineralization (Felzer et al., 2011). Our projections did not demonstrate a decrease in the N-limiting condition of the old-growth forest at Watershed 2 in HJA under future climate change scenarios because changes in net N mineralization are small.

4.3. Potential contribution of increasing atmospheric CO₂ concentration to future water, carbon and nitrogen dynamics

Experimental studies have demonstrated the potential for CO₂ fertilization effects associated with increases in water-use efficiency and photosynthetic rate under elevated atmospheric CO₂ concentrations, despite the considerable debate on whether Rubisco activity and leaf N content will decrease under prolonged exposure to elevated CO₂ concentrations (Ainsworth and Long, 2005; Leakey et al., 2009; Long et al., 2004). Our projections of diminished stomatal conductance with potential CO₂ fertilization effects are consistent with observations from a four-year manipulation experiment using Douglas-fir seedlings (Lewis et al., 2002). However, the long-term combined effects of elevated CO₂ concentrations and increasing temperature on stomatal conductance

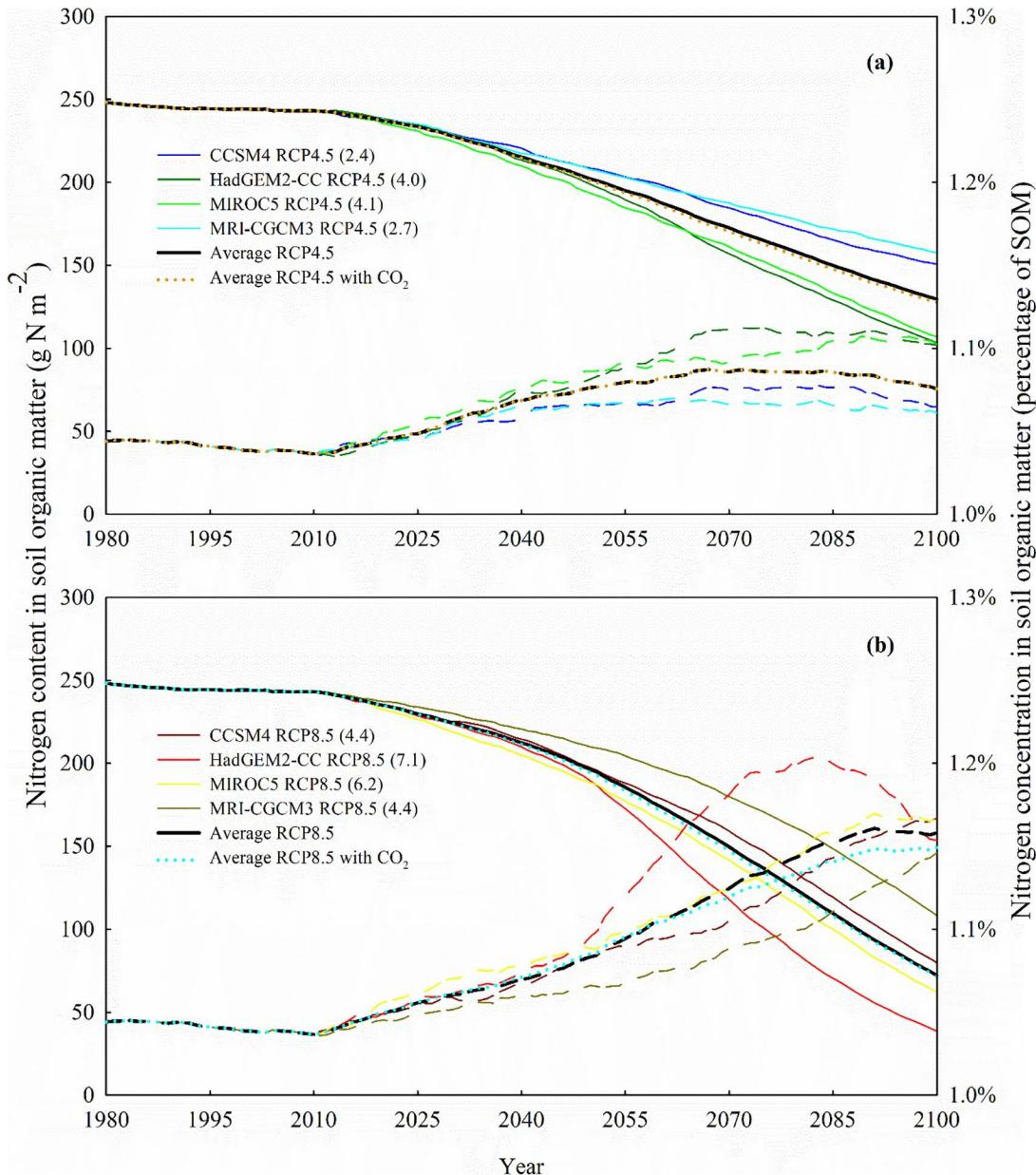


Fig. 9. Past simulations (1980–2010) and future projections (2011–2100) of nitrogen content (solid lines) and nitrogen concentration (dash lines) in soil organic matter under the RCP4.5 (a) and RCP8.5 (b) scenarios for Watershed 2 at the H. J. Andrews Experimental Forest. Projections shown used climate inputs from four GCMs. The values in parentheses for GCM labels indicate increases in annual mean temperature ($^{\circ}\text{C}$) from 1986–2010 to 2076–2100.

projected in our simulations are in contrast with the patterns observed by Lewis et al. (2002) in a short-term experiment. Since Watershed 2 is not projected to suffer from soil moisture stress under future climate change, elevated CO_2 concentration is not likely to affect future foliar display in the old-growth Douglas-fir forest. However, invoking potential CO_2 fertilization effects does result in higher future leaf C assimilation at Watershed 2 except for December. Our projections during the growing season are consistent with findings from a CO_2 enrichment experiment for Douglas-fir seedlings (Lewis et al., 2001). The additional C sequestered due to elevated CO_2 concentration transfers into plant internal storage (PlantC), increasing wood production. Potential fertilization effects of elevated CO_2 concentration on photosynthesis increase NEP compared with projections without CO_2 effects. The only exception to this pattern under potential CO_2 fertilization effects on vegetation occurs by the end of the century when NEP does not increase under the RCP8.5 scenarios because photosynthesis is limited by foliar display, not leaf C assimilation, when foliar biomass is low and atmospheric CO_2 concentration is above

600 ppm (Ollinger et al., 2009). The old-growth forest at Watershed 2 is characterized by low rate of transfer from dead wood biomass to SOM (Table S1), and total litter is largely contributed by foliar and root litter which are not projected to be affected by potential CO_2 fertilization effects. CO_2 fertilization may increase decomposition of SOM by increasing soil moisture associated with increases in water-use efficiency of plants (Felzer et al., 2011). However, such an effect of elevated CO_2 is negligible at Watershed 2 because of low rates of transpiration in the old-growth Douglas-fir forest. As a result, the overall effect of CO_2 fertilization on SOC at Watershed 2 is negligible under the RCP scenarios. Recent studies report elevated CO_2 -enhanced SOM decomposition by mycorrhizal fungi in Free-Air Carbon dioxide Enrichment (FACE) experiments (Cheng et al., 2012; Phillips et al., 2012). However, PnET-BGC does not include this mechanism, and shows negligible effect of CO_2 on future dynamics of SOM. The potential contribution of CO_2 fertilization on future C cycling reported in this study agrees with Hartman et al. (2014) who found the live plant biomass C pool is greater under high CO_2 than low CO_2

scenarios. Potential effects of CO₂ fertilization on future N cycling are not evident. This pattern contrasts with projections using the DayCent-Chem model (Hartman et al., 2014) in which CO₂ effects caused lower nitrogen mineralization and stream NO₃[−] fluxes.

5. Conclusions

This study provides insights into the role of climate change on physiological stress in the dynamics of water, C, and N under the RCP scenarios in an old-growth Douglas-fir forest with Mediterranean climate. Different from previous studies, which observed and projected severe soil moisture stress in the Pacific Northwest, our projections indicate that future air temperature and humidity stress to the vegetation have large impacts on ecosystem functions. The moderate water holding capacity and low demand of transpiration are projected to mitigate against soil moisture stress in the old-growth Douglas-fir forest during the dry growing season. Despite large increases in stomatal conductance from 1986–2010 to 2076–2100 during all months, decreases in foliar NPP and foliar biomass due to the air temperature and humidity stress are projected to decrease transpiration. As a result, future increases in soil moisture are anticipated in summer and fall since little change in precipitation was projected in these seasons. Model projections also suggest future decreases in photosynthesis and C storage in the plant biomass and soil organic matter under the high radiative forcing scenario. Potential CO₂ effects on vegetation are projected to amplify decreases in transpiration and increases in soil moisture in summer and fall, but alleviate future decreasing trends in photosynthesis and live plant biomass under the high radiative forcing scenario. Despite the large quantity of C loss from the ecosystem, climate change is projected to alter foliar and soil N concentrations with little loss from the ecosystem because of the large amount of N uptake by the old-growth Douglas-fir forest. Although projected increases in foliar N concentration only have minor contribution to C assimilation, future increasing N concentration in SOM may alleviate the decrease in net N mineralization despite the reduction in SOM decomposition by the end of the century, while stream N concentrations are expected to remain low. Our findings of severe air temperature and humidity stress under the RCP scenarios demonstrate the central role of changing foliar biomass on future dynamics of water, C, and N in the old-growth forest of the region with Mediterranean climate.

Acknowledgements

We thank Habibollah Fakhraei and Steven Perakis for constructive discussion during the development of the manuscript. Funding for this study was provided by U.S. Environmental Protection Agency through the STAR program (R834188) and Department of Civil and Environmental Engineering at Syracuse University. Data for model calibration and validation were provided by the Pacific Northwest Permanent Sample Plot Program and the H. J. Andrews Experimental Forest research program, funded by the National Science Foundation's Long-Term Ecological Research Program (DEB1440409; DEB0823380), U.S. Forest Service Pacific Northwest Research Station, and Oregon State University. The authors thank Robert Pabst for providing the data on primary production and plant nutrient concentrations, and the editor and three reviewers for their constructive comments and suggestions.

Appendix A. Supplementary data

Supplementary data to this article can be found online at <https://doi.org/10.1016/j.scitotenv.2018.11.377>.

References

- Aber, J.D., 1992. A generalized, lumped-parameter model of photosynthesis, evapotranspiration and net primary production in temperate and boreal forest ecosystems. *Oecologia* 92, 463–474.
- Aber, J.D., Ollinger, S.V., Federer, C.A., Reich, P.B., Goulden, M.L., Kicklighter, D.W., Melillo, J.M., Lathrop, R.G., 1995. Predicting the effects of climate change on water yield and forest production in the northeastern United States. *Clim. Res.* 5, 207–222.
- Aber, J.D., Reich, P.B., Goulden, M.L., 1996. Extrapolating leaf CO₂ exchange to the canopy: a generalized model of forest photosynthesis compared with measurements by Eddy correlation. *Oecologia* 106, 257–265.
- Aber, J.D., Ollinger, S.V., Driscoll, C.T., 1997. Modeling nitrogen saturation in forest ecosystems in response to land use and atmospheric deposition. *Ecol. Model.* 101, 61–78.
- Aber, J.D., Goodale, C.L., Ollinger, S.V., Smith, M., Magill, A.H., Martin, M.E., Hallett, R.A., Stoddard, J.L., 2003. Is nitrogen deposition altering the nitrogen status of northeastern forests? *Bioscience* 53, 375–389.
- Ainsworth, E.A., Long, S.P., 2005. What have we learned from 15 years of free-air CO₂ enrichment (FACE)? A meta-analytic review of the responses of photosynthesis, canopy properties and plant production to rising CO₂. *New Phytol.* 165, 351–371.
- Allen, C.D., Macalady, A.K., Chenchoune, H., Bachelet, D., McDowell, N., Vennetier, M., Kitzberger, T., Rigling, A., Breshears, D.D., Hogg, E.H., Gonzalez, P., Fensham, R., Zhang, Z., Castro, J., Demidova, N., Lim, J.-H., Allard, G., Running, S.W., Semerci, A., Cobb, N., 2010. A global overview of drought and heat-induced tree mortality reveals emerging climate change risks for forests. *For. Ecol. Manag.* 259, 660–684.
- Battaglia, M., Beadle, C., Loughhead, S., 1996. Photosynthetic temperature responses of *Eucalyptus globulus* and *Eucalyptus nitens*. *Tree Physiol.* 16, 81–89.
- Beedlow, P.A., Lee, E.H., Tingey, D.T., Waschmann, R.S., Burdick, C.A., 2013. The importance of seasonal temperature and moisture patterns on growth of Douglas-fir in western Oregon, USA. *Agric. For. Meteorol.* 169, 174–185.
- Berner, L.T., Law, B.E., 2015. Water limitations on forest carbon cycling and conifer traits along a steep climatic gradient in the Cascade Mountains, Oregon. *Biogeosciences* 12, 6617–6635.
- Berntsen, C.M., Rothacher, J., 1959. A Guide to the H. J. Andrews Experimental Forest. USDA Forest Service, Portland, OR (21 p.).
- Berry, J., Bjorkman, O., 1980. Photosynthetic response and adaptation to temperature in higher plants. *Annu. Rev. Plant Physiol.* 31, 491–543.
- Bierlmaier, F.A., McKee, A., 1989. Climatic summaries and documentation for the primary meteorological station, H.J. Andrews Experimental Forest, 1972 to 1984. Department of Agriculture, Forest Service, Pacific Northwest Research Station, Portland, OR, p. 56.
- Bindoff, N.L., Stott, P.A., AchutaRao, K.M., Allen, M.R., Gillett, N., Gutzler, D., Hansingo, K., Hegerl, G., Hu, Y., Jain, S., Mokhov, I.I., Overland, J., Perlitz, J., Sebbari, R., Zhang, X., 2013. Chapter 10 – detection and attribution of climate change: from global to regional. In: Stocker, T.F., Qin, D., Plattner, G.-K., Tignor, M., Allen, S.K., Boschung, J., Nauels, A., Xia, Y., Bex, V., Midgley, P.M. (Eds.), *Climate Change 2013: The Physical Science Basis. Contribution of Working Group I to the Fifth Assessment Report of the Intergovernmental Panel on Climate Change*. Cambridge University Press, Cambridge, United Kingdom and New York, NY, USA.
- Boisvenue, C., Running, S.W., 2006. Impacts of climate change on natural forest productivity – evidence since the middle of the 20th century. *Glob. Chang. Biol.* 12, 862–882.
- Bond-Lamberty, B., Thomson, A., 2010. Temperature-associated increases in the global soil respiration record. *Nature* 464, 579–582.
- Braswell, B.H., Sacks, W.J., Linder, E., Schimel, D.S., 2005. Estimating diurnal to annual ecosystem parameters by synthesis of a carbon flux model with eddy covariance net ecosystem exchange observations. *Glob. Chang. Biol.* 11, 335–355.
- Burns, R.M., Honkala, B.H., 1990. *Silvics of North America: Volume 1. Conifers*. Campbell, J.L., Sun, O.J., Law, B.E., 2004. Supply-side controls on soil respiration among Oregon forests. *Glob. Chang. Biol.* 10, 1857–1869.
- Cheng, L., Booker, F.L., Tu, C., Burkey, K.O., Zhou, L., Shew, H.D., Rufty, T.W., Hu, S., 2012. *Arbuscular mycorrhizal fungi increase organic carbon decomposition under elevated CO₂*. *Science* 337, 1084–1087.
- Clarke, L., Edmonds, J., Jacoby, H., Pitcher, H., Reilly, J., Richels, R., 2007. Scenarios of greenhouse gas emissions and atmospheric concentrations, *Synthesis and Assessment Product: Climate Change Science Program and the Subcommittee on Global Change Research*, Washington, U.S., p. 154.
- Collins, M., Knutti, R., Arblaster, J., Dufresne, J.-L., Fichefet, T., Friedlingstein, P., Gao, X., Gutowski, W.J., Johns, T., Krinner, G., Shongwe, M., Tebaldi, C., Weaver, A.J., Wehner, M., 2013. Chapter 12 - long-term climate change: projections, commitments and irreversibility. In: IPCC (Ed.), *Climate Change 2013: The Physical Science Basis. Contribution of Working Group I to the Fifth Assessment Report of the Intergovernmental Panel on Climate Change*. Cambridge University Press, Cambridge, United Kingdom and New York, United States.
- Coops, N.C., Waring, R.H., 2011. Estimating the vulnerability of fifteen tree species under changing climate in Northwest North America. *Ecol. Model.* 222, 2119–2129.
- Coops, N.C., Hember, R.A., Waring, R.H., 2010. Assessing the impact of current and projected climates on Douglas-fir productivity in British Columbia, Canada, using a process-based model (3-PG). *Can. J. For. Res.* 40 (511–511).
- Daly, C., McKee, W., 2013. *Meteorological Data From Benchmark Stations at the Andrews Experimental Forest, 1957 to Present. Long-Term Ecological Research. Forest Science Data Bank, Corvallis, OR*.
- Dixon, K.W., Lanzante, J.R., Nath, M.J., Hayhoe, K., Stoner, A., Radhakrishnan, A., Balaji, V., Gaitán, C.F., 2016. Evaluating the stationarity assumption in statistically downscaled climate projections: is past performance an indicator of future results? *Clim. Chang.* 135, 395–408.
- Drugokencky, E.J., Lang, P.M., Mund, J.W., Crotwell, A.M., Crotwell, M.J., Thoning, K.W., 2016. *Atmospheric Carbon Dioxide Dry Air Mole Fractions From the NOAA ESRL Carbon Cycle Cooperative Global Air Sampling Network, 1968–2015*.
- Dong, Z., Driscoll, C.T., Campbell, J.L., Pourmokhtarian, A., Stoner, A.M.K., Hayhoe, K., 2018. Projections of Water, Carbon, and Nitrogen Dynamics Under Future Climate Change in an Alpine Tundra Ecosystem in the Southern Rocky Mountains Using a Biogeochemical Model: *Science of the Total Environment*.

- Dyrness, C.T., 1969. Hydrologic Properties of Soils on Three Small Watersheds in the Western Cascades of Oregon. Pacific Northwest Forest and Range Experiment Station, U.S. Forest Service.
- Fakhraei, H., Driscoll, C.T., Renfro, J.R., Kulp, M.A., Blett, T.F., Brewer, P.F., Schwartz, J.S., 2016. Critical loads and exceedances for nitrogen and sulfur atmospheric deposition in Great Smoky Mountains National Park, United States. *Ecosphere* 7, e01466.
- Fakhraei, H., Driscoll, C.T., Kulp, M.A., Renfro, J.R., Blett, T.F., Brewer, P.F., Schwartz, J.S., 2017. Sensitivity and uncertainty analysis of PnET-BGC to inform the development of total maximum daily loads (TMDLs) of acidity in the Great Smoky Mountains National Park. *Environ. Model. Softw.* 95, 156–167.
- Felzer, B.S., Cronin, T.W., Melillo, J.M., Kicklighter, D.W., Schlosser, C.A., Dangal, S., 2011. Nitrogen effect on carbon-water coupling in forests, grasslands, and shrublands in the arid western United States. *J. Geophys. Res. Biogeosci.* 116, G03023.
- Gbondo-Tugbawa, S.S., Driscoll, C.T., Aber, J.D., Likens, G.E., 2001. Evaluation of an integrated biogeochemical model (PnET-BGC) at a northern hardwood forest ecosystem. *Water Resour. Res.* 37, 1057–1070.
- Gilttrap, D.L., Li, C., Saggard, S., 2010. DNDC: a process-based model of greenhouse gas fluxes from agricultural soils. *Agric. Ecosyst. Environ.* 136, 292–300.
- Green, D.G., Sadedin, S., 2005. Interactions matter-complexity in landscapes and ecosystems. *Ecol. Complex.* 2, 117–130.
- Griesbauer, H.P., Green, D.S., 2010a. Assessing the climatic sensitivity of Douglas-fir at its northern range margins in British Columbia, Canada. *Trees* 24, 375–389.
- Griesbauer, H.P., Green, D.S., 2010b. Regional and ecological patterns in interior Douglas-fir climate-growth relationships in British Columbia, Canada. *Can. J. For. Res.* 40, 308–321.
- Hartman, M.D., Baron, J.S., Clow, D.W., Creed, I.F., Driscoll, C.T., Ewing, H.A., Haines, B.D., Knoepp, J., Lajtha, K., Ojima, D.S., Parton, W.J., Renfro, J., Robinson, R.B., Van Miegroet, H., Weathers, K.C., Williams, M.W., 2009. DayCent-Chem simulations of ecological and biogeochemical processes of eight mountain ecosystems in the United States. *U.S. Geol. Surv. Sci. Investig. Rep.* 174.
- Hartman, M.D., Baron, J.S., Ewing, H.A., Weathers, K.C., 2014. Combined global change effects on ecosystem processes in nine U.S. topographically complex areas. *Biogeochemistry* 119, 85–108.
- Hawk, G., Dyrness, C.T., 1972. Vegetation and soils of watersheds 2 and 3, H. J. Andrews Experimental Forest. Coniferous Forest Biome Internal Report. University of Washington, Seattle, WA, p. 48.
- Hay, L.E., LaFontaine, J., Markstrom, S.L., 2014. Evaluation of statistically downscaled GCM output as input for hydrological and stream temperature simulation in the Apalachicola-Chattahoochee-Flint River basin (1961–99). *Earth Interact.* 18, 1–32.
- Hermann, R.K., 1987. North American tree species in Europe. *J. For.* 85, 27–32.
- Janssen, P., Heuberger, P., 1995. Calibration of process-oriented models. *Ecol. Model.* 83, 55–66.
- Jiang, Y., Kim, J.B., Still, C.J., Trugman, A.T., Kim, Y., 2018. Linking tree physiological constraints with predictions of carbon, water, and energy fluxes at an old-growth coniferous forest. *Ecosphere* (in review).
- Jørgensen, S.E., Bendoricchio, G., 2001. *Fundamentals of Ecological Modelling*. Elsevier, New York.
- Kang, S., Running, S.W., Kimball, J.S., Fagre, D.B., Michaelis, A., Peterson, D.L., Halofsky, J.E., Hong, S., 2014. Effects of spatial and temporal climatic variability on terrestrial carbon and water fluxes in the Pacific Northwest, USA. *Environ. Model. Softw.* 51, 228–239.
- Katsuyama, M., Shibata, H., Yoshioka, T., Yoshida, T., Ogawa, A., Ohte, N., 2009. Applications of a hydro-biogeochemical model and long-term simulations of the effects of logging in forested watersheds. *Sustain. Sci.* 4, 179–188.
- Latta, G., Temesgen, H., Adams, D., Barrett, T., 2010. Analysis of potential impacts of climate change on forests of the United States Pacific Northwest. *For. Ecol. Manag.* 259, 720–729.
- Leakey, A.D., Ainsworth, E.A., Bernacchi, C.J., Rogers, A., Long, S.P., Ort, D.R., 2009. Elevated CO₂ effects on plant carbon, nitrogen, and water relations: six important lessons from FACE. *J. Exp. Bot.* 60, 2859–2876.
- Lewis, J.D., Olszyk, D., Tingey, D.T., 1999. Seasonal patterns of photosynthetic light response in Douglas-fir seedlings subjected to elevated atmospheric CO₂ and temperature. *Tree Physiol.* 19, 243–252.
- Lewis, J.D., Lucash, M., Olszyk, D., Tingey, D.T., 2001. Seasonal patterns of photosynthesis in Douglas fir seedlings during the third and fourth year of exposure to elevated CO₂ and temperature. *Plant Cell Environ.* 24, 539–548.
- Lewis, J.D., Lucash, M., Olszyk, D.M., Tingey, D.T., 2002. Stomatal responses of Douglas-fir seedlings to elevated carbon dioxide and temperature during the third and fourth years of exposure. *Plant Cell Environ.* 25, 1411–1421.
- Lewis, J.D., Lucash, M., Olszyk, D.M., Tingey, D.T., 2004. Relationships between needle nitrogen concentration and photosynthetic responses of Douglas-fir seedlings to elevated CO₂ and temperature. *New Phytol.* 162, 355–364.
- Littell, J.S., Peterson, D.L., Tjoelker, M., 2008. Douglas-fir growth in mountain ecosystems: water limits tree growth from stand to region. *Ecol. Monogr.* 78, 349–368.
- Littell, J.S., O'Neill, E.E., McKenzie, D., Hicke, J.A., Lutz, J.A., Norheim, R.A., Elsner, M.M., 2010. Forest ecosystems, disturbance, and climatic change in Washington state, USA. *Clim. Chang.* 102, 129–158.
- Littell, J.S., McKenzie, D., Kerns, B.K., Cushman, S., Shaw, C.G., 2011. Managing uncertainty in climate-driven ecological models to inform adaptation to climate change. *Ecosphere* 2, 1–19.
- Long, S.P., Ainsworth, E.A., Rogers, A., Ort, D.R., 2004. Rising atmospheric carbon dioxide: plants FACE the future. *Annu. Rev. Plant Biol.* 55, 591.
- Manzoni, S., Jackson, R.B., Trofymow, J.A., Porporato, A., 2008. The global stoichiometry of litter nitrogen mineralization. *Science* 321, 684–686.
- Moore, G.W., Bond, B.J., Jones, J.A., Phillips, N., Meinzer, F.C., 2004. Structural and compositional controls on transpiration in 40- and 450-year-old riparian forests in western Oregon, USA. *Tree Physiol.* 24, 481–491.
- Mote, P., Snover, A.K., Dalton, M.M., 2013. *Climate Change in the Northwest: Implications for our Landscapes, Waters, and Communities*. Island Press, Washington.
- NADP, 2016. *National Atmospheric Deposition Program (NRSP-3)*. Champaign, IL.
- Ollinger, S.V., Goodale, C.L., Hayhoe, K., Jenkins, J.P., 2009. Potential effects of climate change and rising CO₂ on ecosystem processes in northeastern U.S. forests. *Mitig. Adapt. Strateg. Glob. Chang.* 14, 101–106.
- Olszky, D., Wise, C., Vaness, E., Tingey, D., 1998. Elevated temperature but not elevated CO₂ affects long-term patterns of stem diameter and height of Douglas-fir seedlings. *Can. J. For. Res.* 28, 1046.
- Ormrod, D.P., Lesser, V.M., Olszky, D.M., Tingey, D.T., 1999. Elevated temperature and carbon dioxide affect chlorophylls and carotenoids in Douglas-fir seedlings. *Int. J. Plant Sci.* 160, 529–534.
- Perakis, S.S., Sinkhorn, E.R., 2011. Biogeochemistry of a temperate forest nitrogen gradient. *Ecology* 92, 1481–1491.
- Phillips, R.P., Meier, I.C., Bernhardt, E.S., Grandy, A.S., Wickings, K., Finzi, A.C., Knops, J., 2012. Roots and fungi accelerate carbon and nitrogen cycling in forests exposed to elevated CO₂. *Ecol. Lett.* 15, 1042–1049.
- Pourmokhtarian, A., 2013. *Biogeochemical Modeling of the Response of Forest Watersheds in the Northeastern U.S. to Future Climate Change*. Syracuse University, Syracuse, NY (167 p).
- Pourmokhtarian, A., Driscoll, C.T., Campbell, J.L., Hayhoe, K., 2012. Modeling potential hydrochemical responses to climate change and increasing CO₂ at the Hubbard Brook Experimental Forest using a dynamic biogeochemical model (PnET-BGC). *Water Resour. Res.* 48, W07514.
- Pourmokhtarian, A., Driscoll, C.T., Campbell, J.L., Hayhoe, K., Stoner, A., 2016. The effects of climate downscaling technique and observational data set on modeled ecological responses. *Ecol. Appl.* 26, 1321–1337.
- Pourmokhtarian, A., Driscoll, C.T., Campbell, J.L., Hayhoe, K., Stoner, A.M.K., Adams, M.B., Burns, D., Fernandez, I., Mitchell, M.J., Shanley, J.B., 2017. Modeled ecohydrological responses to climate change at seven small watersheds in the northeastern United States. *Glob. Chang. Biol.* 23, 840–856.
- Prescott, C.E., Chappell, H.N., Vesterdal, L., 2000. Nitrogen turnover in forest floors of coastal Douglas-fir at sites differing in soil nitrogen capital. *Ecology* 81, 1878–1886.
- Randall, D.A., Wood, R.A., Bony, S., Colman, R., Fichefet, T., Fyfe, J., Kattsov, V., Pitman, A., Shukla, J., Srinivasan, J., Stouffer, R.J., Sumi, A., Taylor, K.E., 2007. Chapter 8 – climate models and their evaluation. In: Solomon, S., Qin, D., Manning, M., Chen, Z., Marquis, M., Averyt, K.B., Tignor, M., Miller, H.L. (Eds.), *Climate Change 2007: The Physical Science Basis. Contribution of Working Group I to the Fourth Assessment Report of the Intergovernmental Panel on Climate Change*. Cambridge, United Kingdom and New York, NY, USA. Cambridge University Press, pp. 589–662.
- Reich, P.B., 2014. The world-wide 'fast-slow' plant economics spectrum: a traits manifesto. *J. Ecol.* 102, 275–301.
- Riahi, K., Grübler, A., Nakicenovic, N., 2007. Scenarios of long-term socio-economic and environmental development under climate stabilization. *Technol. Forecast. Soc. Chang.* 74, 887–935.
- Richardson, A.D., Hollinger, D.Y., Aber, J.D., Ollinger, S.V., Braswell, B.H., 2007. Environmental variation is directly responsible for short- but not long-term variation in forest-atmosphere carbon exchange. *Glob. Chang. Biol.* 13, 788–803.
- Ripullone, F., Grassi, G., Lauteri, M., Borghetti, M., 2003. Photosynthesis-nitrogen relationships: interpretation of different patterns between *Pseudotsuga menziesii* and *Populus × euroamericana* in a mini-stand experiment. *Tree Physiol.* 23, 137–144.
- Rupp, D.E., Abatzoglou, J.T., Hegewisch, K.C., Mote, P.W., 2013. Evaluation of CMIP5 20th century climate simulations for the Pacific Northwest USA. *J. Geophys. Res.-Atmos.* 118, 10,884–10,906.
- Ryan, M.G., 1991. A simple method for estimating gross carbon budgets for vegetation in forest ecosystems. *Tree Physiol.* 9, 255–266.
- Sacks, W., Schimel, D., Monson, R., 2007. Coupling between carbon cycling and climate in a high-elevation, subalpine forest: a model-data fusion analysis. *Oecologia* 151, 54–68.
- Saltelli, A., Tarantola, S., Campolongo, F., Ratto, M., 2004. *Sensitivity Analysis in Practice: A Guide to Assessing Scientific Models*. John Wiley & Sons, Hoboken, NJ.
- Saltelli, A., Ratto, M., Tarantola, S., Campolongo, F., 2005. *Sensitivity analysis for chemical models*. *Chem. Rev.* 105, 2811–2827.
- Saxe, H., Cannell, M.G.R., Johnsen, Ø., Ryan, M.G., Vourlitis, G., 2001. Tree and forest functioning in response to global warming. *New Phytol.* 149, 369–399.
- Shaw, D., Franklin, J., 2017. Long-term Growth, Mortality and Regeneration of Trees in Permanent Vegetation Plots in the Pacific Northwest, 1910 to Present. Long-Term Ecological Research, Forest Science Data Bank, Corvallis, OR.
- Sherwood, S.C., Ingram, W., Tsushima, Y., Satoh, M., Roberts, M., Vidale, P.L., O'Gorman, P.A., 2010. Relative humidity changes in a warmer climate. *J. Geophys. Res.-Atmos.* 115, D09014.
- Smith, S.J., Wigley, T.M.L., 2006. Multi-gas forcing stabilization with Minicam. *Energy J.* 27, 373–391.
- Spittlehouse, D.L., 2003. Water availability, climate change and the growth of Douglas fir in the Georgia Basin. *Can. Water Resour. J.* 28, 673.
- Stoner, A., Hayhoe, K., Yang, X., Wuebbles, D.J., 2013. An asynchronous regional regression model for statistical downscaling of daily climate variables. *Int. J. Climatol.* 33, 2473–2494.
- Taylor, K.E., Stouffer, R.J., Meehl, G.A., 2012. An overview of CMIP5 and the experiment design. *Bull. Am. Meteorol. Soc.* 93, 485–498.
- Thorn, A.M., Xiao, J., Ollinger, S.V., 2015. Generalization and evaluation of the process-based forest ecosystem model PnET-CN for other biomes. *Ecosphere* 6, art43–27.
- Tingey, D.T., Lee, E.H., Waschmann, R., Johnson, M.G., Rygiewicz, P.T., 2006. Does soil CO₂ efflux acclimate to elevated temperature and CO₂ during long-term treatment of Douglas-fir seedlings? *New Phytol.* 170, 107–118.

- Tingey, D.T., Lee, E.H., Phillips, D.L., Rygiewicz, P.T., Waschmann, R.S., Johnson, M.G., Olszyk, D.M., 2007. Elevated CO₂ and temperature alter net ecosystem C exchange in a young Douglas fir mesocosm experiment. *Plant Cell Environ.* 30, 1400–1410.
- Turner, D.P., Conklin, D.R., Bolte, J.P., 2015. Projected climate change impacts on forest land cover and land use over the Willamette River basin, Oregon, USA. *Clim. Chang.* 133, 335–348.
- Unsworth, M.H., Phillips, N., Link, T., Bond, B.J., Falk, M., Harmon, M.E., Hinckley, T.M., Marks, D., Kyaw Tha Paw, U., 2004. Components and controls of water flux in an old-growth Douglas-fir western hemlock ecosystem. *Ecosystems* 7, 468–481.
- Valentine, T., Lienkaemper, G., 2005. 10 Meter Digital Elevation Model (DEM) Clipped to the Andrews Experimental Forest, 1998. Long-Term Ecological Research. Forest Science Data Bank, Corvallis, OR.
- Valipour, M., Driscoll, C.T., Johnson, C.E., Battles, J.J., Campbell, J.L., Fahey, T.J., 2018. The application of an integrated biogeochemical model to simulate dynamics of vegetation, hydrology and nutrients in soil and streamwater following a whole-tree harvest of a northern hardwood forest. *Sci. Total Environ.* 645, 244–256.
- van Vuuren, D.P., Edmonds, J., Kainuma, M., Riahi, K., Thomson, A., Hibbard, K., Hurtt, G.C., Kram, T., Krey, V., Lamarque, J.F., Masui, T., Meinshausen, M., Nakicenovic, N., Smith, S.J., Rose, S.K., 2011. The representative concentration pathways: an overview. *Clim. Chang.* 109, 5–31.
- Wallman, P., Svensson, M., Sverdrup, H., Belyazid, S., 2005. ForSAFE—an integrated process-oriented forest model for long-term sustainability assessments. *For. Ecol. Manag.* 207, 19–36.
- Waring, R.H., Franklin, J.F., 1979. Evergreen coniferous forests of the Pacific Northwest. *Science* 204, 1380–1386.
- Warren, J.M., Meinzer, F.C., Brooks, J.R., Domec, J.C., 2005. Vertical stratification of soil water storage and release dynamics in Pacific Northwest coniferous forests. *Agric. For. Meteorol.* 130, 39–58.
- Way, D.A., Oren, R., 2010. Differential responses to changes in growth temperature between trees from different functional groups and biomes: a review and synthesis of data. *Tree Physiol.* 30, 669–688.
- Wharton, S., Schroeder, M., Bible, K., Falk, M., Paw U, K.T., 2009. Stand-level gas-exchange responses to seasonal drought in very young versus old Douglas-fir forests of the Pacific Northwest, USA. *Tree Physiol.* 29, 959–974.
- Wieder, W.R., Cleveland, C.C., Smith, W.K., Todd-Brown, K., 2015. Future productivity and carbon storage limited by terrestrial nutrient availability. *Nat. Geosci.* 8, 441–U35.
- Wise, M., Calvin, K., Thomson, A., Clarke, L., Bond-Lamberty, B., Sands, R., Smith, S.J., Janetos, A., Edmonds, J., 2009. Implications of limiting CO₂ concentrations for land use and energy. *Science* 324, 1183–1186.
- Woodruff, D.R., Meinzer, F.C., 2011. Water stress, shoot growth and storage of non-structural carbohydrates along a tree height gradient in a tall conifer. *Plant Cell Environ.* 34, 1920–1930.
- Wright, I.J., Reich, P.B., Westoby, M., Ackerly, D.D., Baruch, Z., Bongers, F., Cavender-Bares, J., Chapin, T., Cornelissen, J.H.C., Diemer, M., Flexas, J., Garnier, E., Groom, P.K., Gullas, J., Hikosaka, K., Lamont, B.B., Lee, T., Lusk, C., Midgley, J.J., Navas, M.L., Niinemets, U., Oleksyn, J., Osada, N., Poorter, H., Poot, P., Prior, L., Pyankov, V.I., Roumet, C., Thomas, S.C., Tjoelker, M.G., Veneklaas, E.J., Villar, R., 2004. The worldwide leaf economics spectrum. *Nature* 428, 821–827.